People's Democratic Republic of Algeria
Ministry of Higher Education and Scientific Research
Mohamed Khider University - Biskra

Order Number: .....
Series: .....

Faculty of Science and Technology
Industrial Chemistry Department

THESIS

In Candidacy for the Degree of

DOCTOR 3rd CYCLE IN CHEMICAL PROCESSES

***Option**: Chemical engineering*

By

SALEM SEGHIR

TITLE

Development of predictive models for flocculation processes (Application in papermaking) Développement de modèles prédictifs pour les processus de floculation (Application à la fabrication du papier)

Defended on:
In front of the jury composed of:

Mr. MERZOUGUI Abdelkarim	*Professor at the University of Biskra*	***President***
Mr. HASSEINE Abdelmalek	*Professor at the University of Biskra*	***Supervisor***
Mrs. MARIA GRAÇA Rasteiro	*Professor at the University of Coimbra*	***Co-supervisor***
Mr. MADANI Hakim	*Professor at the University of Batna 2*	***Examiner***
Mr. FADEL Ammar	*Professor at the University of Biskra*	***Examiner***

To my family, whose unwavering love and support have been my foundation throughout this journey . . .

Acknowledgements

My sincere thanks go to my advisor **Pr. Abdelmalek HASSEINE** for his patience, noble guidance and support in accomplishing this work. He has been giving me encouragement and valuable suggestions for these past five years. Thank you very much **Pr. HASSEINE** .

My heartfelt thanks to **Professor Graça Rasteiro** for her invaluable assistance, guidance, and support throughout my research project and particularly during my ERASMUS stay at the University of Coimbra.

My sincere acknowledegments go to **Pr. Abdelkrim MERZOUGUI**, **Pr. Hakim MADANI** and **Pr. Ammar FADEL** who have been so kind to accept to be members of the jury and to read my work.

ملخص

في هذه الدراسة، نستخدم نهجين متميزين ضمن نمذجة التوازن السكاني ثنائي الأبعاد لتوضيح ديناميكيات تألق جزيئات *PCC* عند معالجتها باستخدام *polyelectrolytes* . في هذا التحليل، يقارن نموذج تقنية المحور الثابت بالنموذج الذي وصفه هونسلو في البداية (١٩٨٨) ثم صقله سبايسر وبراتسينيس (١٩٩٦ب). بالإضافة إلى ذلك، تتم مقارنة متوسط أحجام التدفق المقاسة باستخدام تشتت حيود الضوء (*LDS*) مع التنبؤات التي قدمتها هذه النماذج لتقييم دقتها وقابليتها للتطبيق. للتأكد من دقة النماذج في تمثيل النتائج التجريبية، نستخدم مقياس جـدنسس اف ذت (*GoF*) ، مما يؤدي باستمرار إلى قيم تتجاوز ٩٨% في جميع الحالات. من خلال تحسين معايير التركيب بشكل متكرر المرتبطة بكفاءة الاصطدام، ومعدل التجزئة، وإعادة هيكلة *flocs* ، فإننا ننشئ ارتباطات مع خصائص *polyelectrolytes* المستخدمة. بعد ذلك، نشارك في مناقشة شاملة حول تطور حركية التألق وتشتت بيانات الأس بمرور الوقت، كما هو مستمد من جهود النمذجة لدينا. تضع هذه المناقشة هذه النتائج في سياق المشهد الأوسع لعملية التنظيف، مع مراعاة العوامل ذات الصلة مثل خصائص متعدد الكهروتروليت والظروف التجريبية المختلفة. من خلال هذا التحليل متعدد الأوجه، نقدم رؤى حول التفاعل المعقد بين ديناميكيات العملية والسمات الجزيئية، مما يسهل فهمًا أعمق لظواهر التلطيف.

الكلمات المفتاحيّة: التوازن السكاني، تقنية المحور الثابت، نموذج هونسلو، ديناميكيات التكتل، إعادة هيكلة *Flocs* ، صناعة الورق

Abstract

In this study, we employ two distinct approaches within two-dimensional population balance modeling to elucidate the flocculation dynamics of PCC particles when treated with polyelectrolytes. In this analysis, the fixed pivot technique model is compared with the model initially described by Hounslow (1988) and later refined by Spicer and Pratsinis (1996b). Additionally, the median floc sizes measured using Light Diffraction Scattering (LDS) are compared with the predictions made by these models to evaluate their accuracy and applicability. To ascertain the fidelity of the models in representing experimental outcomes, we utilize a Goodness of Fit (GoF) metric, consistently yielding values exceeding 98% across all instances. By iteratively optimizing fitting parameters associated with collision efficiency, fragmentation rate, and flocs restructuring, we establish correlations with the characteristics of the polyelectrolytes employed. Subsequently, we engage in a comprehensive discussion surrounding the evolution of flocculation kinetics and scattering exponent data over time, as derived from our modeling efforts. This discussion contextualizes these findings within the broader landscape of the flocculation process, accounting for pertinent factors such as polyelectrolyte properties and varying experimental conditions. Through this multifaceted analysis, we provide insights into the intricate interplay between process dynamics and molecular attributes, facilitating a deeper understanding of flocculation phenomena.

Key words: Population balance, Fixed pivot technique, Hounslow model, Flocculation dynamics, Flocs restructuring, Papermaking

Résumé

Dans cette étude, nous employons deux approches distinctes à l'intérieur de la modélisation de l'équilibre de la population en deux dimensions pour éclaircir la dynamique de floculation des particules de PCC lorsqu'elles sont traitées avec des polyélectrolytes. Dans cette analyse, le modèle technique de pivot fixe est comparé au modèle initialement décrit par Hounslow (1988) et plus tard raffiné par Spicer et Pratsinis. (1996b). En outre, les tailles moyennes des flocons mesurées à l'aide de la diffraction lumineuse (LDS) sont comparées avec les prédictions faites par ces modèles pour évaluer leur exactitude et leur applicabilité. Pour vérifier la fidélité des modèles dans la représentation des résultats expérimentaux, nous utilisons une métrique Goodness of Fit (GoF), produisant de façon constante des valeurs dépassant 98% dans tous les cas. En optimisant de façon itérative les paramètres d'ajustement associés à l'efficacité de collision, au taux de fragmentation et à la restructuration des flocons, nous établissons des corrélations avec les caractéristiques des polyelétrolytes employés. Par la suite, nous nous engageons dans une discussion approfondie autour de l'évolution de la cinétique de la floculation et de la dispersion des données exponentielles au fil du temps, comme le découle de nos efforts de modélisation. Cette discussion contextualisera ces résultats dans le contexte plus large du processus de floculation, en tenant compte de facteurs pertinents tels que les propriétés du polyeléctrolyte et les conditions expérimentales variables. Grâce à cette analyse multidimensionnelle, nous fournissons des informations sur l'interaction complexe entre la dynamique des processus et les attributs moléculaires, ce qui facilite une compréhension plus approfondie des phénomènes de floculation.

Mots clés : Bilan de population, Pivot fixe, Modele de Hounslow, dynamique de floculation, Restruction des flocs, Fabrication du papier

Table of contents

List of figures

List of tables

Nomenclature

dF mass fractal dimension

Greek Symbols

AFM atomic force microscope

α_{ij} collision efficiency between aggregates in i and j intervals

AKD alkyl ketene dimer

α_{max} maximum collision efficiency

ASA alkenyl succinic anhydride

β_{ij} collision frequency between aggregates in i and j intervals (cm^3/s)

$C-PAM$ cationic polyacrylamide

CFS canadian standard freeness

$CSLM$ confocal scanning laser microscopy

DCS dissolved and colloidal susbstances

DDA dynamic drainage analyser

DDJ dynamic drainage jar

ε average energy dissipation rate (m^2/s^3)

εbi critical energy dissipation rate (m^2/s^3)

$FBRM$ focus beam reflectance microscopy

γ fitting parameter for ddF/dt

GW Gess/Weyerhauser

xi_{ij} Breakage distribution function

LDS laser diffraction spectroscopy

μ fluid viscosity (Pa.s)

$MBDT$ moving belt drainage tester

μ fluid kinematic viscosity (m^2/s)

PAE polyamideamine epichlorohydrine

PAM polyacrylamide

PBE population balance equations

PCC precipitated calcium carbonate

PEI polyethyleneimine

PEO polyethyleneoxide

PFR phenol formaldehyde resin

$poly-DADMAC$ poly-diallyldimethylammonium

$SALLS$ small-angle laser light scattering

SR Schopper-Riegler

τ shear stress (N/m^2)

ζ zeta potential (mV)

Other Symbols

$d0$ characteristic diameter for the class i=1

Di characteristic diameter of the class i (cm)

$dp50$ median particle size (mm).

$dp90$ particle size for which 90 % of the material has a size equal or higher to this value(mm)

G average shear rate (s^{-1})

k_B Boltzmann constant (J/K)

k_c constant ≈ 1

m consistency index

N number of primary particles in an aggregate

n behaviour index

Ni number concentration of flocs containing $2^{i-1} particles (\#/cm^3)$

$r0$ primary particle radius (cm)

Rc effective capture radius (cm)

Rg radius of gyration (nm)

SE scattering exponent

Si fragmentation rate of flocs in i interval (s^{-1})

Std sterror standard error

T absolute temperature (K)

t time (s)

V volume of primary particle (cm^3)

Vi volume of flocs in i interval

x, y fitting parameters for aij

Acronyms / Abbreviations

B fitting parameter for fragmentation rate

C collision efficiency factor for t=0

$d43$ volume mean size(mm)

D fitting parameter for da/dt

$dFmax$ maximum mass fractal dimension

$dp10$ particle size for which 10 % of the material has a size lower or equal to this value

Introduction

The papermaking industry has undergone various efforts to stay competitive, primarily by boosting productivity and cutting costs while maintaining or enhancing product quality [1, 2]. Moreover, contemporary objectives include addressing the environmental impact to ensure process sustainability [2–4].

Increasing machine speed to enhance productivity can lead to more frequent breaks in the paper web, while efforts to reduce water consumption could lead to increased levels of dissolved and colloidal materials in process water [2, 4]. Additionally, the increased use of recycled fibers can introduce contaminants into the furnish, exacerbating production challenges such as deposits, foaming, and reduced retention and paper strength [2–4].

To mitigate the effect the of water closure and higher machine speeds, it is crucial to introduce more effective chemical additives to enhance retention and improve the properties of the sheet, thereby boosting productivity and maintaining system cleanliness [3]. Furthermore, new additives, including sizing compounds, anti-foaming agents, colorants, and antimicrobial agents are continuously introduced to enhance paper quality, although this adds complexity to the wet-end chemistry [3]. However, unretained additives may accumulate in process water, posing environmental concerns.

Addressing challenges in the papermaking industry involves reducing wet-end disruptions and impurities in recycled water, often achieved by enhancing the performance of additives. Since paper web breaks can result from destabilization of retention and drainage stages, optimizing chemical additives is crucial for improving overall process efficiency [2].

to gain a comprehensive understanding of the behavior of flocculated pulp suspensions and their impact on retention and drainage effectiveness, it is imperative to delve deeper into flocculation mechanisms. Flocculation stands as a critical phenomenon in the wet-end phase of papermaking, closely aligned with one of the industry's key strategic focuses: optimal control of the wet-end stage. Achieving optimization in retention chemical usage necessitates a thorough comprehension of flocculation mechanisms, their temporal evolution, their reliance on processing conditions, characteristics of the pulp, and the type of polymer system used.

Extensive research has been conducted on the flocculation processes induced by polymeric additives, with numerous studies elucidating these phenomena and their effects [1, 3–17]. However, in the context of the papermaking process, only a limited number of studies have explored the dynamics of flocculation and the properties of flocs concerning retention, drainage, and sheet formation across different process conditions and with a range of retention aid systems [4, 18–22]. For example, Alfano and colleagues [20] observed an inverse correlation between the mean chord length of flocs measured by scanning laser microscopy and the turbidity of filtrate obtained from dynamic drainage jar testing. Dunham et al. [19] conducted flocculation measurements using focused beam reflectance measurement (FBRM) to explore the relationship between aggregation of cellulosic fibers and drainage rates in dynamic drainage analysis. They also investigated the effect of polyelectrolytes on the distribution of dissolved and colloidal substances (DCS) and how this impacts drainage rates. Their findings suggested that the presence of dissolved and colloidal substances (DCS) negatively impacts both flocculation and drainage processes. When cationic polyacrylamide (CPAM) is used, but the addition of diallyldimethylammonium chloride (DADMAC) improves flocculation by neutralizing the DCS. However, this improvement was not observed in drainage, possibly due to the the creation of particulate complexes that hinder drainage. Comprehending the relationship between floc properties and retention, drainage, and sheet formation is essential

for predicting and optimizing retention and drainage performance, as well as guaranteeing the formation and quality of the sheet. Given that flocculation mechanisms and floc characteristics are predominantly determined by the properties of polymers and the choice of retention aid systems plays a pivotal role in aligning papermaking industry objectives with current trends.

The main purpose of using retention aids is to enhance the attachment of fines and additives to larger fibers, thereby improving particle retention within the paper sheet and boosting drainage efficiency. This process is crucial for optimizing the wet-end stage, reducing contaminants in the water system, and increasing the operational speed of the paper machine. Critical factors such as kinetics, floc structure and strength, and the ability to reflocculate are essential for assessing the effectiveness of retention aid systems, particularly in the context of the high speed and turbulence encountered in paper machines.

Rapid flocculation kinetics are imperative due to the brief interaction window, typically lasting only seconds to milliseconds. Additionally, the resulting flocs must exhibit resilience and possess a strong reflocculation ability to withstand the turbulent conditions inherent in paper machine operation. Furthermore, optimal floc properties are essential for drainage improvement, as excessively large flocs are challenging to dewater. Reversible flocculation is essential for efficient dewatering, as demonstrated by Lindström et al. [23] and Swerin et al. [13], who discovered that employing microparticles systems significantly enhances reflocculation, leading to the formation of smaller and denser flocs, thus enhancing both retention and drainage efficiency. Moreover, the formation of small and uniform floc structures is critical for improving dewatering, particularly in vacuum dewatering processes, as highlighted by Scott [24].

Recent studies have identified branched polyelectrolytes as a promising option for retention aids in papermaking. Research conducted by Shin and colleagues [18, 21] shows that branched polymers form small flocs that exhibit excellent resistance to shear forces,

especially when used in conjunction with microparticles, thus improving their refloccula-tion capabilities. Moreover, branched polymers outperform traditional linear polymers in terms of retention efficiency, without compromising sheet properties even with increased filler content. Furthermore, Brouillette et al. [17, 25] have shown that the effectiveness of branched polymers improves with increased levels of turbulence, resulting in enhanced retention and reduced drainage time. This property could be particularly advantageous for faster paper machines experiencing elevated turbulence during paper formation. Additionally, The utilization of branched polymers does not affect sheet formation performance, and the necessary polymer dosage decreases with higher levels of shearing, compared to traditional linear polymers.

In summary, the utilization of branched polymers as retention aids not only enhances filler retention without detracting from the quality of the final product but also enhances overall papermaking efficiency, particularly in high-turbulence environments.

To reduce production costs and mitigate issues associated with increased contaminants in process water, a deeper understanding of the mechanisms of flocculation using branched polyelectrolytes across different processing settings is needed, considering existing knowl-edge of wet-end chemistry and the evolving landscape of the papermaking industry. This entails evaluating the impact of water properties on flocculation, deflocculation, and refloccu-lation processes, especially those mediated by branched polyelectrolytes, and exploring how microparticle retention aid systems can enhance the effectiveness of polymers, especially branched ones. Additionally, correlating information

on flocculation processes and floc characteristics with retention and drainage outcomes is essential for better comprehension and control of the wet-end stage. Furthermore, under-standing the flow behavior of flocculated particles and correlating rheological informations with flocculation characteristics is crucial. Developing a model capable of describing the

flocculation process and predicting aggregate characteristics under set operating conditions or determining conditions leading to desired performance is imperative.

The thesis is structured into three chapters, we start with an introduction and Chapter 1 providing the littirature review. Chapter 2 describes the evaluation and monitoring of flocculation. Specifically, Chapter 3 focuses on the modeling of the flocculation process. Lastly, the conclusion presents conclusions and recommendations for future research.

Investigating the rheological flow behavior of flocculated suspensions with chemical additives is vital for optimizing energy usage in papermaking, since chemical flocculation influences the mechanical flocculation of fiber suspension. Despite its importance, there are limited studies that have explored how chemical flocculation affects the flow behavior of pulp suspensions, emphasizing the need for further investigations. Understanding and controlling the flocculation process by polyelectrolytes necessitates a quantitative model capable of describing flocculation under varied processing conditions, beyond a single type of additive, thus serving as a valuable tool for modeling the wet-end stage of the paper machine.

Hence, the primary objectives of this thesis involve devising a strategy to collect data on flocculation kinetics, floc resistance, characteristics, and reflocculation, capacity in turbulent conditions, and assessing how polyelectrolyte characteristics influence flocculation dynamics and outcomes.

Chapter 1

Literature Review

1.1 Introduction

In a typical paper machine configuration, it is customary to delineate six distinct sections: the headbox, wire section, press section, drying, surface finnishing treatment, and converting. Figure 1.1 provides an illustration of paper machine of Fourdrinier, wherein these aforementioned sections are discernible. The wet-end segment of inside the machine encompasses the headbox, wire section or forming, and the section for press. Here, the damp papers are shaped and there is water throughout these stages. On the other hand, the drying and surface treatment segments, collectively known as the dry-end part, facilitate the drying of the damp papers generated in the wet-end phase, along with the application of various paper surface treatments [26]. The papermaking process commences with a diluted solution comprising cellulosic fibers, additives, and fillers [26–28]. Additives in papermaking serve two primary purposes: process additives, which optimize machine operation (e.g., defoamers,retention aids, biocides,and dispersants), and functional additives, which alter paper properties (such as wetting agents, dyes, sizing agents, fillers, and optical brighteners). These constituents collectively contribute to shaping the ultimate characteristics of the paper product.

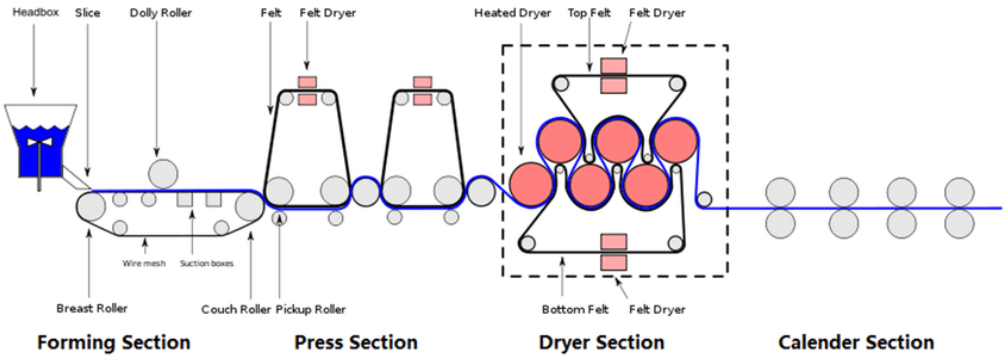

Fig. 1.1 Fourdrinier paper machine

In the papermaking process, additives are pivotal in improving paper properties. Process additives, like retention aids, biocides, dispersants, and defoamers, are introduced at the wet-end of the paper machine. Meanwhile, functional additives, such as dry-strength additives, can be incorporated internally or applied onto the sheet's surface. [29]. In the past, paper manufacturing typically involved acidity, primarily because of the inclusion of rosin and aluminum sulfate for sizing purposes. Nonetheless, from the 1970s onward, there has been a notable transition in the industry towards neutral and alkaline methods. Adopting alkaline systems has brought about several advantages, such as minimizing corrosion, facilitating increased filler incorporation, and conserving energy during the drying process. Within acidic systems, sizing agents like alkenyl succinic anhydrides (ASA) and alkyl ketene dimers (AKD) have taken the place of rosin and aluminum sulfate, as noted by Roberts in 1991. During the papermaking process, the pulp mixture moves from the headbox section to the wire section, where substantial water extraction happens through vacuum application. The consistency rises from 0.2-1.5% in the headbox to 18-23% by the end of the forming section and further to 33-50% in the press section. Following the final drying stage, the sheet achieves approximately 92-96% consistency [30].

The wet-end segment plays a pivotal role in shaping paper structure, with physicochemical interactions among fibers, fines, fillers, and additives shaping paper properties. Flocculation, a crucial aspect of the wet-end process, entails the creation of flocs containing fibers, fines,

fillers, and additives within the pulp suspension. Fibers intertwine mechanically, aiding their retention on the wire section. However, fine particles, being smaller than the wire mesh, require effective retention aids and well-managed flocculation procedures. [26, 31–33].

The process of flocculation entails the creation of flocs, which are composed of fibers, fillers, fines, and additives within the composition suspension. Fibers become interlocked mechanically, aiding in their retention in the wire section [31]. Nonetheless, the presence of larger holes in the wire makes it difficult to mechanically retain small particles effectively.

Numerous studies [34–38] have highlighted the impact of unflocculated fine particles on drainage resistance, impeding water flow through the web [34, 35, 38], Certain researchers[39–41]. have observed that unattached fine particles, when freely moving through the web during dewatering, tend to obstruct water channels, as depicted in Figure 1.2. Therefore, the utilization of chemical additives is crucial for achieving fines and fillers retention, as illustrated in Figure 1.2.

Research on wet-end chemistry has unveiled diverse retention and flocculation mechanisms, which will be thoroughly explored in section 1.2.1. These mechanisms are contingent upon factors such as the specifications and dosage of flocculants, pH levels, the conductivity of water, temperature and the properties of fines, fillers, as well as process parameters like shear forces and residence time. [32, 36, 42]

Assessing flocculation is vital for managing the wet-end stage effectively. The degree of flocculation and the attributes of flocs play a pivotal role in retention, drainage efficiency, and the overall ultimate of the final product quality [27, 30, 4].

In the current context, achieving ideal monitor of the wet-end section is becoming increasingly crucial. Papermakers are embracing strategies aimed at enhancing competitiveness, many of which directly affect the wet-end. For instance, the adoption of measures such as increasing paper machine speeds and the trend toward greater white water recirculation are actively being implemented.

Recent studies have primarily focused on enhancing productivity and reducing costs in papermaking [1, 2]. The advent of high-speed machines has heightened the importance of factors such as kinetics, floc structure, strength, and reflocculation ability, all of which are crucial for efficient retention systems due to the brief interaction time, typically spanning from seconds to milliseconds [36]. Moreover, the properties of flocs are significantly influenced by shear forces [27, 5, 43].Environmental advancements, such as reduced water consumption, result in increased dissolved and colloidal material in process water, consequently impacting retention aid systems and altering flocculation kinetics and floc properties [4, 2, 3].

Recognizing these changes in wet-end chemistry is paramount since adjustments in paper machine operations can impact the effectiveness of retention and drainage additives. The foremost aim of achieving ideal wet-end monitoring is to improve retention and dewatering performance while safeguarding sheet formation integrity. This guarantees superior retention, drainage, and formation characteristics, culminating in a paper sheet boasting exceptional printing and optical attributes. The research endeavors to understand how flocculation mechanisms and ensuing floc properties evolve over time under diverse process conditions, all geared towards boosting productivity, cutting costs, and upholding the standards of top-tier paper products.

1.2 Drainage and retention in papermaking

1.2.1 Chemical aspects of retention

Chemical interactions provide the foundation for a deeper comprehension of the performance of papermaking drainage additives and retention. Indeed, flocculation in the furnish can be induced by fundamental interaction forms including electrostatic forces, steric interactions, hydrogen bonding, and hydrophobic interactions. When two phases come into contact, such as solid-liquid interfaces, the inonic liquids in the dissolution phase are reorganized within

the system in a organized manner to create the surrounding of electrical double layer. This results in difference of potential formation across the solid-liquid interface [32].

In the double layer, it's possible to identify surface, zeta potentials, and Stern. However, because Stern potentials and surface remain unknown for numerous colloidal systems, the electrical nature of particles are often indirectly assessed through the zeta potential measurement. This value indicates both the amplitude and the charge of particles [36].

Colloidal systems are considered stable if they do not undergo aggregation. Such systems stability, influenced by electrostatic interactions, is elucidated by the theory of DLVO formulated by Derjaguin and Landau (1969) and Verwey and Overbeek (1948). According to this theory, the interaction between particles is determined by the combined effects of repulsive and attractive forces [44]. Figure 1.2 illustrates the interaction curve of total energy resulting from these forces that depending on distance between two charged particles. As particles draw closer, repulsion by electrostatics occurs due to their similar charges, while simultaneously, there's an inherent van der Waals forces attraction.

Steric stabilization serves as another mechanism for colloidal particle stabilization. This occurrence due to adherence between polymer chains and particle surface, extending beyond the electrical double layer. By doing so, they prevent particles from approaching each other, thereby diminishing the van der Waals forces effect [30] .

Aggregation arises when particles within a system become destabilized. One method to induce aggregation involves reducing repulsion forces by adding ions, thereby decreasing the thickness of the electrical double layer or lowering the electrokinetic potential, which leads to particle coagulation. Alternatively, polymeric additives can be employed to form bonds between particles, inducing flocculation within the system [30].

In the context of papermaking, where the furnish comprises numerous negatively charged surfaces (such as fibers, fines, and fillers), the system possesses a high negative surface potential. This results in a strong tendency for cationic additives to adsorb, potentially

destabilizing the system [36]. In the paper machine enhancing the retention of fillers and fines in the wet-end section is attended through the utilization of retention aid systems, which operate through various flocculation mechanisms. In the realm of papermaking, these mechanisms of flocculation are also referred to as retention mechanisms.

1.2.2 Flocculation mechanisms

Particle aggregation or suspension destabilization may happen as a result of the chemical interactions previously discussed. through flocculation mechanisms or coagulation. When aggregation occur, multiple processes occur at the same time: the molecules of polymer adsorb to the particle surface, the polymeric chains adsorbed reconfigure, unstable particles collide to obtain new aggregates, and existing aggregates may break apart [6, 8, 11]. The significance and kinetics of each process depend on various factors such as the characteristics of the flocculant (e.g., charge density,molecular weight,structure, and concentration), properties of the suspended particles (e.g., size and charge density), features of the suspending medium (e.g., conductivity,ph, and ionic charge), turbulence intensity, residence time, ...) [1, 6, 7, 45]. Several studies have demonstrated that based on the retention assistance techniques employed, particle aggregation can occur through patching, bridging,charge neutralization, or complex flocculation mechanisms [4, 32]. This section elaborates on these retention mechanisms, illustrating how they function.

1.2.2.1 Charge neutralisation

Charge neutralization serves as a coagulation mechanism, as aggregation arises from the reduction of repulsive forces between particles. By adding an electrolyte salt or a very low molecular weight polyelectrolyte, the electrical double layer is compressed sufficiently, reducing the repulsion between particles and enabling van der Waals attractive forces to induce coagulation among particles with similar electrostatic charges. The optimal dosage corre-

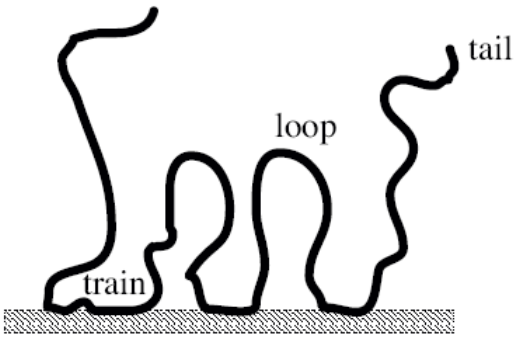

Fig. 1.2 Schematic of polymer chain adsorbed with trains, loops and tails.

sponds to achieving the isoelectric point, beyond which the particles disperse again. Common retention aids that operate via the charge neutralization mechanism include polyvalent cations, polyethyleneimine (PEI), polydiallyldimethylammonium chloride (poly-DADMAC), polyamines, and polyamideamine epichlorohydrine (PAE) [36, 4].

1.2.2.2 Bridging

Bridging-induced flocculation of particles occurs through the action of polyelectrolytes with very high molecular weights (>106). This mechanism was initially proposed by studies conducted by La Mer and Healy (1963), who also noted that the flocculation rate reaches a maximum when the polymer surface coverage is 50%.

The polymer adheres to the particle surface, with its tails and loops extending well beyond the surface. In certain instances, trains may also be present, as depicted in Figure 1.6, which illustrates an example of polymer conformation at the particle surface. Consequently, the particle is capable of interacting with other particles, forming bridges between them, thereby facilitating aggregation, as depicted in Figure 1.7.

Fleer and Scheutjens (1993) outlined the bridging mechanism as comprising three consecutive steps: polymer adsorption, bridging, and depletion.

The conformation of the polymer at the particle surface, along with factors such as polymer thickness and bridging performance, is contingent upon the characteristics of the polymer itself [7, 27].

Furthermore, the suspending medium characteristics also exert influence on bridging flocculation. Numerous studies have demonstrated that these medium properties affect the performance of retention aids [3, 12, 10].

Polyacrylamides or poly (ethylene oxides) of very high molecular weight are examples of retention aids that have been extensively studied and used for flocculation through the bridging mechanism [4] .

Furthermore, aggregates formed via the bridging mechanism tend to be relatively robust. However, excessive shearing can lead to the breakup of these flocs, often referred to as "hard flocs," resulting to the degradation of polymers. Subsequently, when shear forces reduced, the likelihood of reflocculation through the bridging mechanism diminishes, and reflocculation tends to occur instead through the patch mechanism [27, 36] .

1.2.2.3 Complex flocculation

Recently, there have been studies focusing on new retention aid systems aimed at enhancing both retention and drainage in papermaking processes. These systems involve more complex flocculation mechanisms compared to those previously described. Notably, three distinct mechanisms have been identified: dual polymer flocculation, network flocculation and microparticle flocculation.

the combination of a cationic polymer in dual polymer system (e.g., alum, polyethyleneimine, poly-DADMAC, or cationic starch) and an anionic polymer (e.g., anionic polyacrylamide) is employed. Initially, the cationic polymer is introduced to flocculate the anionic particles. Subsequently, the anionic polymer is introduced to reflocculate the flocs, using a bridging mechanism, when a stage of shear is occur [46, 47]. Some studies have demonstrated that

dual polymer systems improve dewaterability, enhance floc strength, and exhibit higher reflocculation capacity compared to single systems [48, 49].

The microparticle system is a subtype of the dual system wherein highly anionic submicron particles (e.g., montmorillonite or colloidal silica) are utilized alongside a cationic polymer such as polyacrylamide or starch. Initially, the cationic flocculant causes particle aggregation. Subsequently, the formed flocs are disrupted when a shear occur, the refloccula-tion of the system is induced by adding subsequently microparticles. The reflocculated flocs are mostly denser and smaller than the originals ones, as illustrated in Figure 1.4 [9, 13] . The microparticle system offers numerous advantages, extensively documented in literature. Swerin and al. [13, 50] provided evidence that microparticle systems exhibit a notable reflocculation capacity, leading to significant enhancements in retention of fines and filler facilitated by polyacrylamides of cationic type. Similarly, other researchers have shown that all these systems concurrently enhance drainage and retention without causing excessive flocculation, which can adversely affect sheet formation [14].

Flocculation network occurs when polyethyleneoxide (PEO) is combined with a phenolic resin. When PEO is used alone, it does not adhere to bleached Kraft fibers or calcium carbonate. Therefore, another compound is necessary to facilitate this interaction. Typically, compounds with aromatic rings, such as phenol formaldehyde resin (PFR), are used for this purpose [51]. It has been proposed that the flocculation mechanism with PEO can form hydrogen bonds with other substances that act as electron acceptors, lead to insoluble complexes between PEO and PFR [15, 51]. However, several additional theories have been proposed by different authors to elucidate the mechanism of flocculation induced by this aid system retention. Lindström and Glad-Nordmark (1984) suggest that PEO and the phenolic resin create a transient and unstable network that encapsulates the fines and fillers particles. Recently, van de Ven and Alince [16] suggested that flocculation takes place through bridges induced by association, where the complex formed by PEO and the phenolic resin acts as

bridges between particles, that ficilitate their aggregation. Similarly, studies conducted by Xiao et al. (1996) to elucidate the retention mechanism proposed a sophisticated bridging model. This model was subsequently validated by Negro et al. (2005), who also demonstrated that the complex induces rapid flocculation of the suspension, resulting in the formation of unstable flocs. These flocs readily reflocculate upon a decrease in shearing.

1.2.3 Elements impact retention mechanisms

As previously mentioned, the wet-end chemistry of papermaking is shaped by a wide array of complex and nuanced elements that require careful management to uphold the production of top-tier final products. This section will provide a deeper exploration of select factors, with a specific focus on their implications for retention mechanisms and, consequently, the characteristics of flocs. These factors encompass:

1.2.3.1 Polymer concentration

The flocculant concentration stands as a pivotal parameter, as it directly impacts The quantity of polymer adsorbed per unit surface of particle represent the rate of adsorption, Tadros [52] introduced the "diffusion-controlled adsorption kinetics model" suggesting when the concentration of polymer surface is below the concentration of equilibrium, while desorption becomes dominant when the surface concentration exceeds equilibrium levels.

Excessive flocculant dosage presents a challenge in papermaking, as precise real-time control proves difficult. Overdosing not only escalates costs but also disrupts the flocculation process and alters floc properties. Blanco and colleagues (2005) investigated the impact of CPAM (cationic type polyacrylamide) overdosing on PCC (precipitated calcium carbonate) flocculation kinetics and floc properties. Their findings indicated that an excess of flocculant heightens repulsive forces between particles, leading to diminished flocculation rates and

hindered particle reflocculation. However, a moderate surplus can enhance the strength and stability of flocs.

1.2.3.2 Polymer charge density

The charge density of a polyelectrolyte significantly impacts its conformation upon adsorption onto the particle surface, thereby determining the primary mechanism of flocculation [7, 27]. Typically, when the molecular weight is high and the charge density is low, the polymer adheres to the particle surface in a manner that extends its tails and loops well beyond the surface, facilitating interaction with other particles. In such cases, bridging bonds largely govern the flocculation process [8, 1].(see section 1.2.3). Furthermore, the adsorbed polymer conformation varies depending on its cationicity: lower cationicity results in the presence of only tails and loops, while higher cationicity may introduce trains as well. Consequently, the bridging capacity decreases at high charge density as polymer chains tend to adopt a flatter conformation on the particle surface. This leads to the formation of cationic patches that attract the polymer-free surfaces of other particles [50, 1]. In such scenarios, the adsorption rate slows down, and the polymer reaches its final conformation earlier, indicating a faster conformation rate with an increasing cationic charge of the polymer.

1.2.3.3 Polymer structure

Alongside charge density, the molecular weight of the polymer plays a substantial role in determining the flocculation mechanism, as elaborated in section 1.2.2. When the polymer's molecular weight is low, the flat shape formed when it adheres to particle surface, thereby facilitating aggregation through the patching process. Conversely, with very high molecular weight, the polymer adopts a more extended conformation, enabling the formation of bridges between particles. The conformation and thickness of the adsorbed polymer layer at the particle surface hinge on both the charge density and the concentration of the polymer.

Additionally, polymer branching constitutes another aspect of polymer structure that influences flocculation performance. While limited studies have examined the conformation of branched polymers at the surface of particle, Nicke and colleagues (1992) showcased the efficacy of a new copolymer with branches, comprising diallyldimethylammonium chloride and triallylmethylammonium chloride, as a flocculant in the paper manufacturing. Similarly, Shin and co-workers (1997a) conducted a comparative analysis of the flocculation efficacy between highly branched cationic polyacrylamides and conventional linear polyacrylamides. Their findings revealed that the highly branched polymer generated smaller flocs with enhanced shear resistance, presenting potential as a retention aid in microparticulate systems. Subsequent research by the same team [18] validated the superior retention efficiency of branched polymers in microparticulate systems, ultimately resulting in improved sheet formation even with increased filler content.

Recent studies conducted by Brouillette et al. [17, 25] have investigated the performance of high-molecular-weight branched cationic polyacrylamide (C-PAM) in combination with a microparticle system under conditions of high turbulence. Their findings indicated that this retention aid system notably improved filler retention, particularly in environments with elevated turbulence levels. Despite a general decline in filler retention with increased turbulence across all polymers, branched polymers exhibited greater resistance to shearing and displayed superior efficiency. Furthermore, the drainage time increased with turbulence for all polymers, with branched polymers yielding the most favorable outcomes. Notably, branched polymers required lower dosages to achieve effective retention as turbulence intensified, presenting potential cost savings. Importantly, the introduction of branching did not compromise sheet formation, which remained satisfactory both linear and branched types of flocculants.

Overall, branched polymers are anticipated to surpass traditional linear flocculants in efficiency on high-speed paper machines generating substantial turbulence levels.

1.2.3.4 Shear forces

Paper machines with High-speed are integral to modern paper manufacturing to stay competitive. Consequently, There is a critical need to enhance retention aid systems. capable of producing enhanced flocs. This is essential due to the importance of the properties of flocs (structure,size, and strength) significantly influence wet-end performance. Research must approach this from two angles, recognizing the very high turbulence induced in the headbox of the paper machine, where flocculation occurs, contrasting with the significantly reduced turbulence in the forming section.Under the intense shear conditions in the headbox, initial flocs form are often fragmented, but partial reflocculation occurs as shear forces diminish in the forming area [49].However, the process of flocculation as well as the dynamics and extent of reflocculation are influenced by the characteristics of the polymer. Indeed, initial floc characteristics, especially structure and size, crucially impact the reflocculation stage [53]. Consequently, understanding both the flocculation and reflocculation processes is essential since the final stage of reflocculation dictates the performance of the wet-end section.

In the flocculation process, shearing emerges as a critical parameter. Besides destabilization, mixing is indispensable for promoting flocculation, since polymer molecules must come into contact with fine particles to adhere, and polymer-coated particles must interact with one another (Gregory, 1985). Therefore, with an increase in shearing, there is a rise in the frequency of particle collisions, leading to an enhanced rate of flocculation [36]. However, as flocs grow larger, their further enlargement is restricted by the applied shear, which erodes or breaks them down depending on their size [54–56]. In fact, the shearing forces that tend to disrupt flocs become more significant as their size increases, thereby reducing the collision efficiency of the particles. Consequently, there exists a limiting size for floc growth, determined by the balance between aggregation and breakage [5, 11, 57]. Generally, the breaking of a floc is categorized as either "surface erosion" or "large-scale fragmentation." Erosion entails the detachment of small particles from the surface of the floc, while fragmentation

involves the breaking apart of the flocs into smaller, comparable-sized pieces. Theoretical models in the literature indicate that particle erosion is caused by shearing stresses on the floc surface, whereas fragmentation is believed to result from pressure gradients throughout the entire floc body [43, 58].

1.2.3.5 Electrolytes and anionic impurities in the suspending medium

Increasing the closure of process water circuits in papermaking is a current trend aimed at reducing water consumption. However, this trend leads to a notable rise in the concentration of inorganic salts in the water, which can significantly impact the performance of retention aids and, consequently, wet-end operations [3, 12, 10, 21, 59, 60].

For instance, Hulkko and Deng (1999) observed a substantial impact of increased electrolyte concentration, resulting from the salting-out effect, on both single cationic polyacrylamide (C-PAM) systems and microparticle retention aid systems. The salting-out effect generally decreases the solubility of organic compounds in the presence of dissolved salts. Stemme et al. (1999) Additionally, it was demonstrated that higher ionic strength impacts the efficiency of microparticle retention aid systems. More recent studies by Stoll and Chodanowski (2002) utilized Monte Carlo simulations to investigate the effect of ionic concentration on the rigidity of polymer chains and their ability to adsorption. They found that reducing chain stiffness or ionic concentration promoted better polymer adsorption. High levels of dissolved inorganic compounds can alter the conformation of polymer chains through the salting-out effect, thereby Decreasing the polymer's ability to bridge between particles [3]. As a result, alterations in polymer conformation, alter floc characteristics and flocculation kinetics. Moreover, it has been observed that increased concentrations of inorganic compounds impact the stability and drainage properties of papermaking systems. Therefore, managing the balance of inorganic salts in process water circuits is essential to optimize wet-end performance and achieve efficient papermaking operations.

1.2.4 Drainage mechanisms

If retention performance is essential for wet-end efficiency, then water removal is also a critical parameter for attaining the desired paper properties, boosting productivity, and reducing costs.

Water is extracted from the fiber suspension and subsequently from the fiber web across three main sections of a paper machine: forming, pressing, and drying. In the forming and wet pressing sections, mechanical methods are used for water removal, while in the drying section, water is eliminated through evaporation.

In paper web The bulk of free water is typically removed in the forming and pressing sections, as illustrated in Figure 1.1. The remaining water is retained within tiny capillary spaces inside or among fibers, and this water can only be extracted in the dryer section [24].

Two primary mechanisms drive In the paper machine, dewatering involves thickening and filtration [54]. Filtration takes place when the suspension is sufficiently diluted, allowing fibers and other suspended elements to move independently. This results in a suspension of consistent density over a fiber web that thickens as filtration progresses. Filtration typically forms a fiber web where fibers lie predominantly in the plane of the sheet, resembling infinitely thin layers. Additionally, filtration dewatering leads to relatively uniform sheets.

Thickening, however, takes place when fibers and other suspended particles are partially immobilized within a network, preventing independent movement during dewatering. Thickening typically produces a more uneven fiber web structure compared to filtration.

In practice, the drainage mechanism in high-speed paper machines involves a interaction of filtration and thickening processes [28]. This often results in a sheet where some fibers are oriented out of the plane or even perpendicular to the plane of the web, which can give the sheet a less homogeneous appearance.

During the sheet forming process, a delicate balance exists between oriented shear and turbulence patterns. Parker [54] proposed that both oriented shear and turbulence are

crucial in draining the wet web. Turbulence helps prevent the creation of a dense, relatively impermeable fiber web near the forming fabric, thereby maintaining an open structure in the sheet for effective drainage. Conversely, oriented shear spreads the fibers along the direction of the main force, influencing the network structure (refer to Figure 1.11).

The wire section of most paper machines is divided into two sections: the suction zone and the forming zone, each contributing to different types of dewatering. Depending on the type of paper machine, dewatering in the forming zone may be accomplished by filtering, thickening, or both [36]. On the other hand, the vacuum causes air to compress the sheet and remove water in the suction zone, where vacuum-assisted dewatering takes place. Compression is the primary governing factor for dewatering in the vacuum-assisted zone, as shown by Unbehend [33]. The primary method for removing water is the wet web's subsequent densification since a thicker web has less room for free water.

As previously discussed regarding retention, flocculation also impacts drainage performance. Unbehend [33] highlighted the numerous parallels between the two methods, indicating that enhancements in retention often lead to enhancements in drainage. Flocculation influences drainage by retaining fines and colloidal substances at fiber surfaces and by increasing the available space for water removal. However, excessive flocculation, resulting in large flocs, can hinder drainage because removing interstitial water from extremely large flocs becomes challenging. When a vacuum-In In the context of vacuum-assisted dewatering, employing polyelectrolytes could result in decreased drainage within the vacuum zone. This can occur due to several factors, such as enhanced sheet porosity or compromised formation due to elevated fines retention [24]. When polyelectrolytes are introduced, water may be quickly replaced by air if air can move through channels in regions of little basis weight in the moist web.

In the papermaking process, selecting the appropriate retention aid systems requires careful consideration. These systems must effectively increase the retention of raw materials

while simultaneously reducing drainage period without adversely affecting sheet formation. Balancing these objectives is crucial to optimizing the efficiency and quality of the papermaking process.

1.2.5 Devices for Measuring Retention and Drainage

1.2.5.1 Indirect methods

Indirect methods are essential for gaining insights into the behavior of chemical agents used throughout the flocculation process, which is crucial for controlling and predicting the wet-end step in papermaking. While and drainage and retention measurements provide valuable information, they do not directly reveal flocculation behavior or floc properties. Therefore, several indirect methods have been developed to address this need.

1. Titration : Titration methods involve determining the optimal flocculant dosage based on the charge neutralization theory, often using indicators such as zeta potential or isoelectric point. However, these methods may not accurately predict the optimal dosage when bridging or patching mechanisms dominate.

2. Zeta Potential Determination: Zeta potential measurement tracks changes in surface charge during flocculation, reflecting transitions between different flocculation mechanisms. It provides insights into polymer conformation and its impact on flocculation kinetics.

3. Turbidity Measurement: Turbidity analysis assesses the flocculation ability by measuring the turbidity of white water, which indicates the presence of colloidal substances. Changes in turbidity reflect variations in the efficiency of flocculation.

4. Settling Tests: Settling tests evaluate flocculant performance by observing settling behavior in the absence of turbulence. This method indirectly provides information

about floc size and structure, such as the mass fractal dimension, under sedimentation conditions.

While these traditional methods offer valuable insights into flocculation behavior and performance, they may have limitations in predicting the behavior of high molecular weight polymers or when complex flocculation mechanisms are involved. Therefore, caution must be exercised when interpreting results from these indirect methods, and they should be complemented with direct observation and analysis techniques for a comprehensive understanding of flocculation processes in papermaking.

1.2.5.2 Direct methods

Various laboratory devices have been created in recent decades for studying retention and drainage in papermaking. Some of these devices allow for the simultaneous determination of drainage rate and sheet properties. Here are descriptions of several existing methods used to evaluate drainage and retention:

1. Tests for Canadian Standard Freeness (CSF) and Schopper-Riegler (SR) Test: These are common methods for determining freeness, which measures the ease of water flow from a fiber suspension. The tests measure the drainage time of a specific volume of water from a given quantity of pulp suspension. Freeness is expressed in milliliters of free water that has been drained in the CFS test and as degrees in the SR test.

2. Dynamic Drainage Jar (DDJ) or Britt Jar: Introduced in 1973, the DDJ is widely used for screening retention aids. It allows for the measurement of retention of fine fibers and fillers in authentic dynamic conditions. Additionally, The DDJ can be utilized to assess drainage by recording the volume of liquid drained over a set period.

3. Laboratory Devices for Vacuum-Assisted Dewatering: These devices simulate vacuum-assisted dewatering, as observed in paper machines, by withdrawing filtrate through a

screen. Examples include the Moving Belt Drainage Tester (MBDT), the Gess/Weyerhauser (G/W) system, and the Dynamic Drainage Analyzer (DDA).

4. MBDT: Introduced in 1992, The MBDT replicates drainage and pulsation on the wire, enabling the modification of vacuum profiles and pulsation frequencies to closely simulate actual conditions on a paper machine.

5. G/W System: Introduced in 1983, the G/W system measures the drainage rate while maintaining a constant volumetric pumping rate of the vacuum pump, providing a characteristic drainage curve.

6. DDA: Introduced in 1990, The DDA assesses drainage and concurrently delivers data on retention and wet sheet permeability. It features a drainage unit coupled with a microprocessor that manages various parameters throughout the testing process.

These laboratory devices help researchers optimize papermaking processes by providing insights into retention, drainage, and sheet properties. The wet sheet formed during testing can also undergo further analysis to evaluate filler and fines retention, formation index, brightness, and resistance using conventional analytical methods.

1.3 Assessment of Flocculation

As observed in the preceding section, most techniques used to understand flocculation mechanisms and, as a result, to control the wet-end stage are based on analyzing particle and aggregate characteristics. Therefore, this section will outline typical aggregate properties used to evaluate flocculation effectiveness and, subsequently, wet-end efficiency. Furthermore, different methods for measuring these properties will be explored.

1.3.1 Characteristics of Aggregates

1.3.1.1 Size distribution

Particles are intricate three-dimensional structures, necessitating three parameters for a comprehensive description. Therefore, a single number cannot fully describe a particle's size. Consequently, many sizing methods assume particles are spherical, as spheres are the only shapes describable solely by diameter. While this simplifies representing particle size distributions, this can result in inaccuracies when measuring non-spherical particles. Figure 1.16 illustrates spherical equivalent diameters determined through different methods, with the choice of diameter depending on the process's relevance (e.g., surface area, volume).

Size distributions can be described in terms of number, volume, mass, or surface area, and are usually displayed as fractional or cumulative distributions across size intervals. Key statistical parameters, such as the mean, median, mode, d10, and d90, are used to characterize these distributions:

Median (d50): Splits the population evenly, where 50% of the particles are larger and 50% are smaller than the median size.

Mode: Indicates the most frequently occurring size within the distribution, marked by the peak of the distribution curve. d10: The particle size below which 10% of the material falls.

d90: The particle size below which 90% of the material falls.

The mean represents the weighted arithmetic average of particle sizes, with various means calculated The representation of particle size distributions varies based on the physical property being measured, such as number, surface area, volume, or mass. This variation requires differentiation between various means, including the arithmetic mean diameter weighted by number d[1,0], by surface area d[3,2], and by volume d[4,3]. Each mean reflects the specific property measured, resulting in distinct formulas for the particle size distribution mean. Equation 1.2 offers a general formula for calculating the mean of a particle size distribution.

$$d[p,q] = \left[\frac{\sum f_c d_c^p}{\sum f_c d_c^q}\right]^{\frac{1}{p-q}} \quad \text{with } p \neq q \tag{1.1}$$

f_c represents The percentage of particles in the size class q refers to the order of distribution, while $(p-q)$ indicates the order of the property being measured. Scattering techniques commonly produce a mean size based on a mass or volume size distribution, typically assumed to be either 1 or 2.

1.3.1.2 Structure

The structure of aggregates holds significant importance in papermaking, as evidenced by the correlation between floc strength, density, and retention and dewatering capabilities. The fractal concept, introduced by Mandelbrot in 1982, has become a valuable tool for quantitatively characterizing aggregate structure.

The mass fractal dimension, denoted as dF, serves as a means of quantifying the extent referring to how primary particles fill the space within the nominal volume of an aggregate, making it a convenient parameter for characterizing floc density [61]. It has been observed that aggregates of colloidal particles exhibit fractal properties [62]. For any mass fractal aggregate, the mass (m) of the aggregate is directly proportional to its radius (R), raised to a power equal to dF, as described by Equation 1.3.

$$\rho(R) \propto R^{d_F - 3} \tag{1.2}$$

This relationship demonstrates that as the floc size (R) increases, the density of the floc decreases. Thus, a larger floc will be less dense than a smaller floc of similar composition. The mass fractal dimension serves as a dependable measure of an aggregate's structural compactness, with typical values ranging from 1 to 3 in three-dimensional Euclidean space. Lower fractal dimension values indicate structures that are more spread out, delicate, and

stringy, while higher values signify structures that are mechanically stronger and more compact [63].

1.3.2 Measurement of aggregate properties

1.3.2.1 Image analysis

Imaging is recognized as one of the oldest and most adaptable techniques for particle characterization. It goes beyond merely measuring aggregate size by offering detailed insights into particle morphology through direct visualization of the aggregates. This method stands in contrast to other techniques that infer size and structure based on theoretical models. Various instruments, such as transmission electron microscopes, optical microscopes, and in situ microscopes, have been utilized to capture images of aggregates. The in situ microscope is particularly valued for its ability to determine floc morphology without the biases introduced by sampling and sample preparation.

In evaluating the fractal dimension of aggregates using 2D images, various analytical methods such as box counting, sandbox, and mass-radius methods are utilized, supported by image processing software. [63]. Bushell and colleagues (2002) noted that image analysis is particularly effective for large, high-contrast particles forming structures with low fractal dimensionality. While existing methods yield reasonably confident results, challenges arise from image processing and limited statistical accuracy due to the particle counting nature of the technique. Nonetheless, this approach offers the advantage of individually examining aggregates, providing insights into structure variability not observable through light scattering techniques. Additionally, impurities can be removed from the analysis, tackling the problem of dust contamination often encountered in light scattering techniques.

Confocal scanning laser microscopy (CSLM) stands out as the sole method capable of addressing the difficulty of projecting three-dimensional structures onto a two-dimensional plane. Thanks to the 3D imaging capabilities of CSLM, calculating the fractal dimension

becomes more feasible using techniques designed for 2D images. Nevertheless, CSLM is limited by its relatively low resolution and challenges associated with multiple scattering [64].

1.3.2.2 Non-scanning laser microscopy

The suite of optical techniques used to monitor flocculation behavior and dynamics in papermaking has grown with the recent addition of non-imaging scanning laser microscopy, also known as focused beam reflectance microscopy (FBRM). An example of this is the Lasentec® FBRM, as shown in Figure 1.19.

FBRM operates by scanning a highly focused laser beam at a constant speed across particles or aggregates in suspension. It detects reflections from these particles, allowing for real-time analysis of particle size and distribution. These reflections are transmitted to a photodiode detector, and the temporal duration of each reflection, multiplied by the velocity of the scanning laser, provides a measurement of the particle geometry known as the chord length. Thousands of chord length measurements are collected per second, generating a histogram where the observed counts are sorted into several chord length bins over the range of 0.5 to 1000 or 2000 mm. Utilizing the FBRM software, one can easily compute and analyze total counts, counts within specific size regions (population), mean chord length, and various other statistical parameters [1].

Research has shown that this technique is highly effective for exploring the flocculation mechanisms of retention aid systems, optimizing flocculant dosages, and assessing floc strength and reflocculation capabilities

1.3.2.3 Light scattering

Light scattering is based on the principle that particles interacting with a laser beam scatter light at angles directly proportional to their size. As the size of the particles decreases, the angle at which they scatter light increases logarithmically. Additionally, the intensity of the

scattered light also varies with particle size, decreasing as the particle volume decreases. Consequently, large particles scatter light at narrow angles with high intensity, while small particles scatter at wider angles but with low intensity [65].

Numerous instruments that use light scattering technology harness this principle to determine particle size. A typical setup, referenced as Figure 1.20, includes a laser that generates a coherent, intense beam of light at a stable wavelength. It also features a series of detectors that track the pattern of light scattered across a broad spectrum of angles. Furthermore, the system incorporates a sample presentation mechanism that ensures the material being tested flows through the laser beam as a homogeneous stream of particles, enabling precise measurements in a known and reproducible state of dispersion. The wavelength of light used for the measurements is also significant, with smaller wavelengths (e.g., blue light sources) offering improved sensitivity to sub-micron particles.

In laser diffraction equipment, particle size distributions are calculated by comparing the scattering pattern of a material with an appropriate optical model. Traditionally, two different models are utilized: the Fraunhofer approximation and the Mie Theory. The Fraunhofer approximation, used in early diffraction instruments, assumes that the particles being measured are opaque and that Light scattering occurs exclusively due to the interaction between the laser beam and the contours of the particles. As a result, this method is suitable only for larger particles and yields inaccurate assessments of the fine particle fraction. On the other hand, the Mie Theory offers a more rigorous solution for calculating particle size distributions from light scattering data. It predicts scattering intensities for all particles, whether small or large, transparent or opaque [65, 66].

The Mie Theory considers primary scattering from the surface of the particle, with intensity predicted by the refractive index difference between the particle and the dispersion medium. It also predicts secondary scattering caused by light refraction within the particle, which is especially important for particles below 50 microns in diameter, as stated in the

international standard for laser diffraction measurements [65]. As mentioned in the previous section, light scattering techniques are valuable for offering insights into aggregate structure by analyzing the scattering patterns.

1.3.3 Rheological properties of flocculated suspensions

The rheological properties of Flocculated suspensions are vital in several phases of the paper-making process, such as the pumping of fiber suspensions and the formation of paper [67]. The behavior of cellulosic fiber networks in suspension exhibits viscoelastic properties, as demonstrated by Wahren (1964) and further explored by Kerekes et al. (1985). This viscoelastic behavior arises from the formation of three-dimensional networks, where fibers change direction under turbulent shear and become trapped within a network structure as they try to return to their original shape.

The development of this three-dimensional network is affected by multiple factors including the consistency of the pulp, length of the fibers, electrostatic charge on the fiber surfaces, hydrodynamic forces, and the ionic strength and pH of the suspending medium [68]. Additionally, chemical flocculants added during paper manufacture facilitate the flocculation of fine fibers and fillers onto fiber surfaces, enhancing their retention in the web [67]. Chemical flocculation impacts the mechanical flocculation of the fiber suspension, which in turn influences the rheological behavior of the entire suspension.

Research suggests that The influence of chemical flocculation on the rheological behavior of pulp suspensions becomes less significant at high pulp consistencies (3% or above) because the strength of the fiber network is already substantial and not significantly enhanced by the flocculant [69]. However, studies have shown that cationic polymers induce flocculation in low consistency fiber suspensions, thereby strengthening the formed network [70, 67].

Despite the importance of flocculation mechanisms in determining floc properties and rheological behavior of suspensions,Only a limited number of studies have directly connected

the flocculation mechanism to the rheological behavior of flocculated fiber suspensions [67, 71]. This lack of understanding is partly due to the limitations of commercial equipment for characterizing such suspensions, primarily due to prevailing aggregation effects. However, Negro et al. (2006) used a rheometer with a unique geometry to bypass these constraints, as detailed later in their study.

1.4 Modelling of flocculation processes

The mathematical representation of flocculation, wherein destabilized suspended particles aggregate, traditionally involves two distinct steps: transport and attachment. The transport step, leading to particle collision, occurs due to local variations in fluid/particle velocities resulting from random thermal motion, imposed velocity gradients from mixing, and differences in settling velocities (perikinetic flocculation, orthokinetic flocculation, and differential sedimentation, respectively). Attachment depends on short-range forces related to surface properties. Mathematically, the rate of successful collision between particles of size i and j is expressed as:rate of flocculation rate of flocculation=ab(i,j)n Here, a is the collision efficiency, b(i,j) is the collision frequency between particles of size i and j, and are the particle concentrations for particles of size i and j, respectively. The collision frequency b depends on the mode of flocculation, while the collision efficiency a reflects the degree of particle destabilization, with higher destabilization yielding higher values of a. Essentially, b measures transport efficiency leading to collisions, while a represents the percentage of those collisions resulting in attachment. Most flocculation models are based on this fundamental equation, with the values of a and b influenced by various factors, including particle nature, destabilization method, and flow regime. Research on flocculation modeling typically concentrates on identifying equations and specific values for these parameters. However, it's crucial to recognize that particle concentration terms also play a significant role in the overall rate, as higher concentrations lead to increased rates. While the interpretation above implies

that b are independent, an alternative interpretation blurs this distinction. In this view, a acts as an experimental correction factor compensating for theoretical representation weaknesses in b, potentially allowing a values beyond the traditional 0 to 1 range.

$$\frac{dn_k}{dt} = \frac{1}{2}\sum_{i+j=k} \beta_{i,j} n_i n_j - \sum_{i=1}^{\infty} \beta_{i,k} n_i n_k \tag{1.3}$$

The subscripts i, j, and k denote discrete particle sizes. In the equation, the first term on the right-hand side represents the increase in particles of size k due to flocculation of two particles whose combined volume equals that of a particle of size k. The second term illustrates the loss of particles of size k resulting from their aggregation with particles of other sizes. The factor of one half preceding the first term ensures that each collision is not counted twice during summation. Overall, the equation defines the rate of change in the number concentration of particles of size k.

By formulating such an equation for each value of k, Smoluchowski developed a set of differential equations that describe the entire flocculation process. These equations are nonlinear, and finding solutions to them is not straightforward. Because solving this equation is not straightforward, Smoluchowski made several basic assumptions. He posited that each collision is entirely successful (aij=1), assumed uniform particle size, and assumed that both particles and aggregates were spherical. Additionally, he assumed binary collisions between particles due to laminar fluid motion, neglecting any floc breakage [56]. Nevertheless, these assumptions significantly limit the analytical solution derived from this traditional method, causing it to diverge from real-world systems.

breckage is considered [56]. However, the analytical solution obtained from this classical approach is substantially limited by these assumptions, and it deviates from real-life scenarios. Consequently, numerous authors have suggested modifications to this equation, and significant advances have been made using numerical techniques to model particle growth through aggregation [56]. For example, a slice method has been developedthat segments

the entire range of particle sizes of interest into a manageable number of size distributions, which simplifies the process of solving the coagulation kinetic equations for tracking the time evolution of the size distribution [72]. Efforts have also been undertaken to incorporate the fracture process into flocculation models. Fair and Gemmell [73] initially incorporated aggregate breakage into their fundamental study of flocculation, highlighting the critical role of breakage within the flocculation system. Recent developments have enhanced the numerical approach by applying a cross-sectional approximation alongside simplified distribution functions to simulate particle flotation. This method takes into account both aggregation and disintegration processes [55, 74, 75]. The particle size distribution has been shown to stabilize in a shock shaking system. Recently, factors such as turbulent shear rate, flocculant dose, primary particle size, and solid fraction have been integrated into population balance equations (PBEs) to model aggregation processes.. and burst at the same time [76]. As emphasized by Thomas and colleagues [56], understanding the fractal dimension is central to better application of flocculation modeling in real systems. Consequently, some authors introduced a fractal dimension to PBEs to model shear-induced flocculation of porous aggregates [67, 77]. These efforts typically assume a consistent structure for all herds throughout the process. In fact, Selomulya and colleagues [78] showed that the flocculent structure undergoes significant changes. Therefore, a change in the structure of flocs was incorporated into the population balance equations (PBEs) by altering the fractal dimension (referred to as the scattering exponent) during the flocculation process.

Furthermore, recognizing that the collision efficiency diminishes with larger aggregate sizes, Kusters et al [79] introduced a model wherein the collision efficiency decreases exponentially with increasing dimensionless floc size, as outlined in Equation 1.1 Kusters et al [79] proposed a model in which the collision efficiency decreases exponentially with the increase in dimensionless floc size, as detailed in Equation 1.4. This efficiency tends towards zero when the size ratio of colliding aggregates is 0.1.

$$\alpha_{ij} = \left[\frac{\exp(-x\left(1-\frac{i}{j}\right)^2}{(i\times j)^y} \right] \times \alpha_{max} \tag{1.4}$$

The variables The classes denoted by i and j are those in which colliding aggregates are located. x and y are fitting parameters and $\alpha_{\max}$ is the high limit of α_{ij}.

i and j denote the size categories in which colliding aggregates are located, $\alpha_{\max}$ represents the upper limit of α_{ij} $(0 \leq \alpha_{\max} \leq 1)$ the fitting values of x and y are used to calculate the collision efficiency with x=y=0.1 and $\alpha_{\max}$=1.

1.4.1 Fixed pivot technique

The FPT (Fixed Pivot Technique) is predicated on the premise that particles within a cell are concentrated at its turning point, commonly referred to as the center of the cell. A newly formed particle with a characteristic u in the size range $[u_i, u_{i+1}]$ is partitioned into cells u_i and u_{i+1} by the fractions. $b_1(u,u_i)$ and $b_2(u,u_{i+1})$, respectively. To ensure that the graph aligns with the two general width properties $X_1(u)$ and $X_2(u)$, these fractions must satisfy the following equations.

$$b_1(u,u_i)_1(u) + b_2(u,u_{i+1})_1(u+1) = X_1(u) \tag{1.5}$$

$$b_1(u,u_i)_2(u) + b_2(u,u_{i+1})_2(u+1) = n_2(u) \tag{1.6}$$

After many algebraic transformations, we obtain the ultimate collection of discrete equations presented as follows:

$$\begin{aligned} \frac{dN_i(t)}{dt} = & \sum^{j\geq k}_{\substack{j,k \\ x_{i-1}\leq x_j+x_k\leq x_{i+1}}} \left(1-\tfrac{1}{2}\delta_{j,k}\right)\eta\,\alpha_{\mathrm{j,k}}\beta_{\mathrm{j,k}}\mathrm{N_j}(t)\mathrm{N_k}(t) \\ & -N_i(t)\textstyle\sum_{k=1}^{M}\alpha_{\mathrm{i,k}}\beta_{\mathrm{i,k}}N_k(t) + \sum_{k=i}^{M} n_{i,k}S_kN_k(t) - S_iN_i(t) \end{aligned} \tag{1.7}$$

The method exhibits several flexible features, yet, as demonstrated by the authors, it tends to overestimate the number density in the larger size range when utilized on coarse grids and exaggerates the higher moments of the distribution. To address this issue of over-prediction in number density, Kumar and Ramakrishna introduced a moving pivot technique [80]. The mathematical formulation of this technique is more intricate and leads to stiff differential equations. For more comprehensive information, readers are directed to the original reference [80].

1.4.2 The discretized model proposed by Hounslow et al. (1988)

The discretized population balance equation, first introduced by Hounslow et al. (1988) and further refined by Spicer and Pratsinis (1996b), has been extensively used to study flocculation processes involving aggregation and breakage. This equation segments the particle size range by doubling the volume of particles or flocs (v_i) at each interval $(v_{i+1} = 2v_i)$, leading to what is referred to as Equation 1.8.

$$\begin{aligned}\frac{dN_i}{dt} = &\sum_{j=1}^{i-2} 2^{j-i+1}\alpha_{i-1,j}\beta_{i-1,j}N_{i-1}N_j + \frac{1}{2}\alpha_{i-1,i-1}\beta_{i-1,i-1}N_{i-1}^2 \\ &- N_i\sum_{j=1}^{i-1} 2^{j-i}\alpha_{i,j}\beta_{i,j}N_j - N_i\sum_{j=i}^{\infty}\alpha_{i,j}\beta_{i,j}N_j - S_iN_i + \sum_{j=i}^{\infty}\Gamma_{i,j}S_jN_j\end{aligned} \tag{1.8}$$

N_i In the context of the population balance equation, represents the number concentration of flocs containing 2^{i-1} particles, with N1 denoting the number concentration of primary particles. Equation 1.20 includes initial terms that illustrate the formation of flocs in size interval i resulting from collisions between flocs from smaller size ranges. The subsequent terms in the equation represent the loss of flocs in interval i due to aggregation with those from other size intervals, as well as losses from fragmentation. Additionally, there are terms accounting for gains from the fragmentation of larger flocs. Parameters $\alpha_{i,j}$ and $\beta_{i,j}$ denote collision efficiency and frequency between flocs in i and j sections, respectively. Additionally,

Si represents the fragmentation rate of flocs in interval i, while $\Gamma_{i,j}$ is the breakage distribution function generating fragments falling in interval i from the break-up of flocs in interval j. Chapter 4 will provide a detailed explanation of the population balance model as expressed by Equation 1.20, which is used in conjunction with Equation 1.15. This discussion will clarify how the model relates to operating conditions and the relevant physicochemical characteristics of primary particles.

Chapter 2

Flocculation assessment and monitoring

2.1 Introduction

Following an initial examination of available methodologies for monitoring flocculation processes, the current research opted for the LDS technique as the chosen method. The findings demonstrate that LDS offers a comprehensive means of evaluating flocculant performance, providing concurrent data on floc size distribution, average size, and mass fractal dimension continuously over time, provided that the equipment is set up for ongoing data collection. Additionally, performing flocculation within the equipment's dispersion unit under controlled turbulent conditions closely mimics real-world process dynamics.

Given the importance of filler retention in papermaking, the flocculation of precipitated calcium carbonate, frequently used as a filler in the papermaking process, was examined under turbulent conditions to serve as a representative model. The study presents and discusses results concerning the flocculation mechanisms of eight different high molecular weight cationic polyacrylamides (C-PAMs), varying in charge densities and branching degrees.

Initially, The study explored the impact of flocculant charge density, degree of branching, and concentration on the size, structure, and flocculation kinetics and mechanisms of flocs. Additionally, zeta potential measurements were conducted throughout the flocculation pro-

cess. Optical microscopy, along with image analysis, was initially used to visualize the shape of flocs at the conclusion of the flocculation process, thereby validating the LDS results.

Subsequently, the application of LDS was expanded to assess deflocculation and reflocculation processes. These processes involved subjecting flocs to sonication at various frequencies (mechanical forces) or increasing shear forces within the test equipment's recirculation tubes (hydrodynamic shearing) was achieved by adjusting the pump speed. An evaluation of the resistance and reflocculation capacity of the flocs was conducted for all the studied C-PAMs.

It's crucial to mention that when initially adapting the LDS (Laser Diffraction Spectroscopy) technique to monitor flocculation processes, experiments involving flocculation, deflocculation, and reflocculation were first carried out using three of the studied C-PAMs (A1++, BHMW, and E1+) at a solid concentration of 0.02% (w/w). These initial findings were discussed in two separate papers [81, 82] and are not detailed in this document. Further preliminary results led to a third publication [83], which assessed the impact of precipitated calcium carbonate (PCC) characteristics on flocculation kinetics.

After the initial stage, the processes of flocculation, deflocculation, and reflocculation were examined at a solid concentration of 0.05% (w/w), which is more representative of the typical suspension concentrations found in the paper industry. In the context of the LDS (Laser Diffraction Spectroscopy) technique, this concentration equates to approximately 70% obscuration, higher than the usual range to ensure signal quality. However, this concentration can be increased during flocculation, as obscuration decreases due to aggregate growth, ensuring the final obscuration falls within the typical analysis range.

Results indicated that flocculant properties similarly, the impact on flocculation, deflocculation, and reflocculation processes for the tested concentrations of precipitated calcium carbonate (PCC) was observed. Subsequently, the focus shifted to examining six polymers

with medium and low charge densities (E1, E1+, E1++++, and E2) to assess their performance under comparable conditions.

The study then explored the impact of water ionic content on flocculation, floc resistance, and reflocculation capacity using industrial white water. This approach was mirrored in experiments using distilled water, which included measurements of zeta potential to further understand the flocculation dynamics. Additionally, the effects of polymer concentration and branching were analyzed, comparing the outcomes in industrial water to those in distilled water. These evaluations were limited to C-PAMs of medium charge density (E1, E1+, E1++++, and E2), as high charge density polymers caused operational issues in the LDS (Laser Diffraction Spectroscopy) equipment, and low charge density polymers required unfeasibly high concentrations for effective results. Some medium and low charge density C-PAMs were also tested in conjunction with complex microparticulate systems.

For tests in distilled water, flocculation was monitored using the LDS technique. After disrupting the flocs through sonication or increased pump speed, microparticles (bentonite) were added to examine the reflocculation capacity of these systems.

Furthermore, the performance of the LDS technique in tracking flocculation processes was compared with the FBRM (Focused Beam Reflectance Measurement) technique, as detailed in existing research on papermaking filler flocculation. At the Universidad Complutense of Madrid, flocculation tests of PCC using the E1s and G1s polymer series were conducted with FBRM equipment. The study assessed floc resistance, reflocculation capacity, and the ability to reflocculate with complex microparticulate systems, comparing these findings with those obtained through the LDS method.

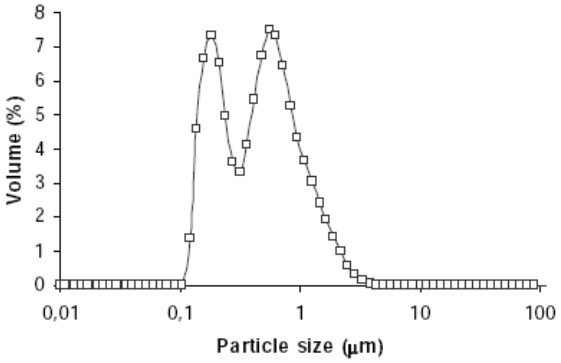

Fig. 2.1 PCC particles size distribution

2.2 Experimental techniques

2.2.1 Materials

2.2.1.1 Precipitated Calcium Carbonate (PCC)

For the flocculation experiments, a commercial scalenohedral precipitated calcium carbonate (PCC) suspension was used. Initially, the PCC particles were dispersed in distilled water and allowed to sit for several days. This step helped remove most of the production additives typically found on the particle surfaces. After this period, the water was drained, and the PCC was dried into a powder form. This process was crucial for maintaining the stability of the PCC suspension during the experiments.

The PCC suspensions were then prepared at a 1% (w/w) concentration in distilled water. For adequate particle dispersion, the suspensions were first stirred magnetically for 20 minutes and then sonicated at 50 kHz for 15 minutes. New batches of PCC suspension were made daily to ensure uniformity in the experimental conditions.

After these preparations, the median particle size, as measured by laser diffraction spectroscopy (LDS), was around 0.5 mm. The pH of the suspension was noted to be 7.5. The zeta potential of the particles was recorded at -30 mV in distilled water. Figure 3.1 displays the size distribution of the precipitated calcium carbonate (PCC) particles.

Table 2.1 Alpine-FlocTM properties

Alpine-FlocTM	Intrinsic Viscosity (mL/g)	Molecular weight (g/mol)	Charge density (%)	Number of Branches
E1	2560	$1.2x10^7$		Linear
E1+	2720	$1.3x10^7$	50	1
E1++++	2515	$1.2x10^7$		4
E2	2640	$1.3x10^7$		4

* determined in 0.05 M NaCl at 20ºC

2.2.1.2 Flocculants

For this study, cationic polyacrylamide (C-PAM) emulsions with very high molecular weights provided by AQUA+TECH were used. The polyelectrolytes employed were characterized primarily by their charge density and degree of branching, as detailed in Table 3.1. Each of these polymer emulsions had a polymer content of about 40% (w/w). Dimethylaminoethyl acrylate was used as the cationic monomer in all polymers. Flocculant solutions were freshly prepared in distilled water at a concentration of 0.1% (w/w) daily to maintain their effectiveness.

2.2.2 Floccualtion monitoring

LDS technique

The monitoring of PCC flocculation was conducted using light diffraction scattering (LDS) with a Malvern Mastersizer 2000. The procedure involved adding the PCC suspension to 700 mL of distilled water in the dispersion unit to achieve 70% obscuration, corresponding to a PCC concentration of about 0.05% (w/w). Tests were performed at a pump speed of 1400 rpm (312 s-1). To ensure the quality of the measurements, [81]. Obscuration levels were kept above 5%, ideally remaining below 20%. Starting tests at 70% obscuration helped maintain obscuration above 5% throughout the test, accommodating any reduction due to floc growth.

Flocculants were tested near their optimal concentrations, determined using a method described by Blanco and colleagues (1996). This involved gradually adding the flocculant to the PCC suspension until no further aggregation occurred, marking the optimal dosage range. The mean aggregate size then stabilized or could potentially decrease due to steric stabilization or electrostatic repulsion. This method provided only an estimated range of optimal dosages, necessitating additional tests to accurately define the effective optimum.

In the doctoral study, the addition of flocculant to the suspension was systematically carried out at dosages near this optimal range. Each trial began by measuring the initial size of PCC particles, followed by the introduction of a set amount of flocculant. Floc size distribution was then monitored at one-minute intervals for 14 minutes until size stabilization was noted.

Offline calculation of the mass fractal dimension of the flocs was done using the scattering pattern from the LDS measurements, based on the Rayleigh-Gans-Debye approximation for particles smaller than 1.0 mm with a refractive index of 1.572. Additionally, the scattering exponent for larger aggregates was derived from the same patterns to reflect the formation of secondary aggregates from primary ones.

Zeta potential (ζ) measurements were taken at three specific intervals: one minute, seven minutes, and fourteen minutes after adding the flocculant, using a Zetasizer NanoZS. Consistent conductivity of the distilled water, maintained between 5 and 8 mS/cm, was crucial as fluctuations could significantly affect flocculation dynamics. Each flocculation test was repeated at least four times for each flocculant concentration.

To confirm these findings, optical microscopy with image analysis (using an Olympus BH-2 microscope and analysSIS 2.11 software) was utilized at the end of the flocculation process to visually inspect floc shapes. Mean floc sizes were calculated until a 95% confidence level was achieved.

2.2.2.1 FBRM technique

Before initiating flocculation tests, the optimal dosage of flocculant was established using a method developed by Blanco et al. (1996), adapted here with the use of the FBRM M500LF system by Lasentec. Following this, flocculation experiments were conducted at flocculant concentrations near this determined optimal level. The procedure involved mixing 30 mL of PCC suspension at a 1% concentration with 120 mL of distilled water in the equipment's beaker, achieving an overall PCC concentration of approximately 0.2% (w/w). The mixture was stirred at 250 rpm. After measuring the initial particle size of the PCC, the flocculant was introduced in one go. Floc sizes were then recorded every 10 seconds for a total duration of 4 minutes.

2.2.3 The resistance of flocs and their ability to reflocculate

The assessment of floc resistance was conducted using two different types of shear forces. Initially, the flocs underwent sonication at two specific frequencies, 10 kHz and 20 kHz, each for 30 seconds. This application of mechanical shear occurred directly in the LDS dispersion unit right after the flocculation process. Following this, a second approach was applied that involved varying hydrodynamic shear forces. This was achieved by gradually increasing the speed of the recirculating peristaltic pump from 1400 rpm to 1800 rpm and then to 2200 rpm over a minute, effectively increasing the shear rate from 312 s^{-1} to 488 s^{-1} and 708 s^{-1} respectively. After both shear tests, the shear force was returned to the original setting to allow for reflocculation, which was then observed for an additional 5 minutes.

At the end of the reflocculation period, both the mass fractal dimension and the scattering exponent for the reflocculated flocs were calculated to assess the structural changes.

2.3 Results and discussion

2.3.1 Flocculation process

2.3.1.1 Optimum flocculant dosage

The diameters of flocs, represented by dp50, in relation to the concentration of polymer included to the PCC suspension were analyzed across a different flocculants. This examination facilitated the identification of optimal concentration ranges for each flocculant, crucial for subsequent experiments. By observing maximum values in dp50 curves, concentration ranges where optimal flocculant dosage could be achieved were delineated. Interestingly, some flocculants displayed simultaneous peaks in both dp50, indicating the optimal concentration is associated with the latter. It's noteworthy that a decrease in dp50 signifies deflocculation, resulting in smaller flocs. The concentration ranges established using Blanco's methodology are summarized in Table 3.1. Additionally, the effective optimum dosage of flocculant corresponds with the dosage identified by LDS, where a specific amount of flocculant is added all at once to the suspension.

Table 2.2 Alpine-FlocTM Properties

	E1	E1+	E1++++	E2
Dosage range (mg/g)	6-8	8-12	6-10	6-10
Effective optimum dosage (mg/g)	8	10	10	8

As anticipated, the rate of flocculation diminishes with increasing concentrations of flocculant beyond the optimal dosage, a phenomenon observed across all polymer types. This decrease in flocculation rate can be attributed to the diffusion-controlled adsorption kinetics model, wherein higher polymer concentrations correspond to reduced rates of polymer adsorption onto particle surfaces [52]. Consequently, the equilibrium point is attained more swiftly at lower flocculant concentrations, resulting in earlier attainment of final floc sizes.

Conversely, at elevated dosages, floc size increases gradually due to the surplus polymer, which intensifies repulsive forces between particles.

When the flocculant dosage falls below the optimum level, floc sizes tend to be smaller owing to reduced efficiency in primary particle collisions, thereby diminishing floc size. Conversely, when polymer dosage exceeds the optimum, floc sizes also remain smaller compared to the optimal dosage.

This phenomenon is attributed to steric stabilization or electrostatic repulsion, which prevents the effective formation of larger flocs.

Additionally, the flocculation kinetics, as depicted in Figures 3.5 to 3.12, show diverse patterns, indicating that the kinetics are influenced by the specific properties of the flocculants, a topic that will be detailed further in upcoming sections. For polymers with medium and low charge densities, there is a noticeable reduction in floc size after a peak is reached, which can be attributed to polymer reconformation (discussed in section 3.3.1.3). This reconformation process is also affected by the concentration of the polymer, which will be elaborated upon in the next section, 3.3.1.3. Notably, at higher flocculant concentrations, polymers experience a slower rearrangement on densely populated surfaces, hindered by the proximity of neighboring molecules, leading to less extensive polymer conformation changes [84, 8].

2.3.1.2 Flocculant dosage effect

Following the establishment of defined concentration ranges for flocculants, a sequence of flocculation tests was performed to pinpoint the optimal dosage for each polyelectrolyte. This dosage was identified as the one that produced the largest flocs with the fastest flocculation kinetics. Once this optimal dosage was determined (as listed in Table 3.2), tests were conducted at this dosage and at both lower and higher concentrations. However, for A1++ and BHMW, testing focused only on the optimum and higher dosages, as initial tests in

a PCC suspension with a 0.02% (w/w) concentration showed these flocculants were less effective for papermaking applications.

The testing sequence for the fourth flocculant illustrated the progression of median floc size over time as it related to polymer concentration. Moreover, the processes of deflocculation and reflocculation were also depicted, with the LDS technique allowing for the simultaneous observation of these three dynamics in a single experiment.

As expected, the rate of flocculation diminished when the concentration of the flocculant exceeded the optimal level for all polymers. This decrease can be explained by the diffusion-controlled adsorption kinetics model, where an increased polymer concentration slows the rate of polymer binding to particle surfaces. As a result, the equilibrium point is achieved more swiftly at lower flocculant concentrations, allowing the final floc size to be reached sooner [52]. Conversely, at higher dosages, the growth of floc size is more gradual due to the abundance of polymer, which intensifies repulsive forces between particles.

When the flocculant dosage is below the optimum, the resulting floc sizes are smaller due to diminished efficiency in primary particle collisions, which leads to smaller flocs. Similarly, when there is an excess of polymer, the floc sizes also tend to be smaller than at the optimum dosage.

2.3.1.3 Flocculant charge density effect

The charge density of the flocculant significantly affects the flocculation mechanism. For the E2 polymer, floc sizes continue to increase until a steady state is achieved. In contrast, for the E1++ polymer and the E1 and E2 series, floc sizes initially grow, reach a peak, and subsequently decline due to aggregate restructuring or breakage.

This pattern, notably seen with the E1 polymer, typifies flocculation triggered by high-charge-density polymers. In such scenarios, polymer chains generally assume a flatter arrangement on particle surfaces. As the charge density lessens, the polymers form tails

and loops that protrude from the surface, enhancing interaction with other particles and promoting flocculation through bridging mechanisms. Once aggregates form, polymer chains might reorganize on the surfaces, leading to a reduction in floc size due to compaction.

Thus, the E1 polymer series, which has medium to low charge densities, primarily supports flocculation via bridging. This bridging effect intensifies as the charge density diminishes.

The optimal dosage of flocculant is also dependent on the polymer's charge density. There is a noticeable trend where the required flocculant dosage increases as the polymer's charge density decreases. This pattern reflects the underlying mechanisms of flocculation: with higher charge densities, polymers can spread more efficiently across particle surfaces, thereby requiring less polymer to achieve optimal coverage. This observation is corroborated by zeta potential measurements (Figure 3.13), which show a decline in zeta potential as polymer charge density decreases, initially starting from a negative charge (-30 mV) on PCC particles that becomes positive after adding the flocculant.

However, determining the optimal flocculant dosage solely based on this parameter would be insufficient as it doesn't fully reveal the flocculation dynamics or kinetics. Additionally, polymer charge density not only affects the kinetics but also the properties of the flocs, such as size and structure.

There is a trend towards forming larger flocs as polymer charge density decreases, driven by the conformation of the polymer on the particle surface, which is largely dictated by its charge density. When polymers are flat against the particle surface, particles within the aggregate are closer together compared to when the polymer adopts a configuration with tails and loops that extend outward, facilitating easier adsorption onto other particle surfaces upon collision and resulting in a greater inter-particle distance.

Both the mass fractal dimension and scattering exponent were calculated at the peaks and at the conclusion of the flocculation kinetics curve, utilizing the light scattering patterns

observed in all experiments. The calculation of scattering exponents is crucial because there is floc restructuring due to polymer reorganization during flocculation, leading to the formation of secondary aggregates from primary ones. Consequently, the Rayleigh-Gans-Debye theory becomes less applicable, making the scattering exponent a necessary metric to accurately depict the fractal nature of the aggregates.

Moreover, floc size distribution was determined using the Mie theory, showing excellent alignment between the data fitting and the optical model, validating the effectiveness of the LDS technique used in this study.

In summary, both fractal dimension (dF) and scattering exponent (SE) values generally decrease with increased flocculant dosage, especially toward the end of the flocculation process, suggesting that flocs become more open at higher concentrations of flocculant. At lower concentrations, polymer molecules rearrange more swiftly. However, on crowded surfaces at higher flocculant concentrations, rearrangement is slower due to interference from adjacent molecules, leading to larger inter-particle distances and the formation of more porous flocs.

2.3.1.4 Flocculant branching effect

When analyzing the E1 polymer series results, it is evident that reconformation is less pronounced in both the linear (E1) and highly branched (E1++++) polymers. Specifically, the flocculation kinetics for the linear polymer are quicker, and it requires less polymer for effective flocculation (as detailed in Table 3.3). Initially, the linear polymer adheres to particle surfaces in a flat configuration, restricting the opportunity for significant polymer chain reconformation, particularly when compared to branched polymers. In the case of the highly branched polymer (E1++++), the polymer's hydrodynamic size, indicated by the radius of gyration, is smaller than that of linear polymers, complicating reconformation

due to the increased density of branches, which reduces the radius of gyration as branching increases.

Moreover, polymer structure impacts the size of the largest flocs observed during the flocculation process (described in Table 3.4). The smallest degree of branching (E1+) produced larger flocs. There isn't a direct correlation between floc size and polymer branching, likely influenced by dynamics such as flocculation kinetics and polymer configuration on particle surfaces. It suggests that floc size is interconnected with polymer structure. Therefore, with the linear polymer adhering in a flatter configuration, it results in smaller flocs because of the reduced space between particles. Conversely, the highly branched polymer, despite its compact structure due to a smaller radius of gyration, maintains small spaces between particles, affecting floc size differently based on the polymer characteristics.

These findings affirm that polymer branching degree significantly influences flocculation dynamics and floc structure. Within the E1 series, mass fractal dimension and scattering exponent measurements at the peak of flocculation indicate denser floc structures for both E1 and E1++++, consistent with the observed trends in floc size. Furthermore, E1++++ produces larger but more open structured flocs than E1, as shown by lower fractal dimension and scattering exponent values for E1++++.

At the conclusion of the flocculation, differences in fractal dimensions are minor, likely due to floc restructuring. However, scattering exponent values are higher for flocs formed with E1+ and lower for E1++++ at optimum dosages. The increase in fractal dimension and scattering exponent during flocculation is minimal for both polymers, indicating limited polymer reconformation. Thus, substantial reconformation can lead to denser flocs, even if initially more open due to bridging.

For the optimal polymer concentration, the largest variance is between the linear and branched polymers. The linear polymer, adhering flatter on particle surfaces, requires a smaller dosage for optimal coverage. For both E1+ and E1++++, higher dosages are

necessary, with E1++++ needing slightly less than E1+. The increased branching in E1++++ likely allows for a more uniform charge distribution, aiding in polymer attachment to particles and requiring a slightly lower dosage than E1+. While bridging dominates in E1++++, the polymer chains protrude less from the particle surface, contributing to a flatter configuration, aligning with the more open structure seen in E1+ aggregates at the flocculation peak.

In contrast, the G1 polymer series does not show the same clear patterns as the E1 series, with the effect of branching degree on floc structure and size being less distinct. Here, the space between particles may be ample enough that branching does not significantly influence flocculation dynamics and floc properties. Nonetheless, the main difference remains in the optimal dosage, which is lower for the linear polymer, reflecting variations in flocculation kinetics and floc characteristics, with dosage requirements being the most notable difference for effective flocculation.

2.3.2 Flocs resistance

Utilizing the LDS (Light Diffraction Scattering) method, it has been noted that floc sizes decrease sharply upon exposure to sonication, suggesting significant floc disintegration. This disintegration occurs because polymer chains detach from particle surfaces, causing the bonds that hold particles together within the aggregate to break. Additionally, floc disintegration becomes more pronounced with increased sonication frequencies due to stronger shear forces. It has also been observed that floc disintegration lessens when there is an excess of polymer, suggesting that flocs may become more robust at polymer dosages exceeding the optimal level. This observation aligns with the research by Negro et al. (2005), which noted that an abundance of polymer enhances the number of polymer links between particles, thereby strengthening the overall structure of the aggregate.

In terms of polymer charge density, there is a noticeable correlation where higher charge densities increase floc resistance, as demonstrated by lower percentages of floc disintegration.

This correlation is explained by the polymer's conformation on particle surfaces; higher charge densities allow polymers to lay flatter against the particle surfaces, enhancing their bonding capability. Conversely, as charge density diminishes, the polymers cannot maintain as flat a configuration, leading to weaker bonds with the particles and consequently, more susceptible floc structures. This effect is corroborated by observations of floc structures, which tend to be more open and less compact as the polymer charge density decreases.

2.3.3 Conclusion

The results obtained in this chapter highlight the benefits of utilizing the LDS (Light Diffraction Scattering) technique for comprehensively evaluating and understanding the flocculation process and determining floc characteristics. The developed experimental methodology enables the acquisition of detailed information on the evolution of floc dimensions and structure over time, as well as the assessment of floc resistance and flocculation kinetics, all within a single integrated test. This approach has led to the identification of the optimum flocculant dosage and a deeper understanding of the underlying flocculation mechanisms, which can be correlated with the mass fractal dimension and scattering exponent of the flocs.

LDS proves to be a valuable tool for assessing the performance of polymeric flocculants, particularly suited for studying flocculation in turbulent environments. The validity of the LDS results is confirmed by the results obtained through image analysis, demonstrating its superiority over traditional techniques like image analysis in determining floc characteristics.

Analysis of flocculation tests involving eight polymers with high molecular weight reveals significant impacts of polymer charge density, polymer structure, and dosage on the flocculation mechanism and floc structure. Flocculation rate decreases and floc structure becomes more open as flocculant concentration increases. Flocculants of low and medium charge density primarily act via the bridging mechanism, while those of high charge density mainly employ the patching mechanism, although the latter's effectiveness may be hindered

by very high molecular weight. The optimum flocculant dosage decreases as polymer charge density increases, resulting in larger and more open flocs with lower charge density polymers.

The branching of high charge density polymers reduces the capacity to form patching bonds, with the optimum flocculant dosage increasing with branching for polymers of medium charge density but slightly decreasing for highly branched polymers. Linear polymers lead to faster flocculation and less pronounced floc restructuring compared to highly branched polymers. Moreover, floc resistance decreases with increasing floc size, while reflocculation is minimal except for linear polymers of high charge density.

Furthermore, LDS successfully investigates deflocculation and reflocculation processes under different conditions such as sonication and increased pump speed, with floc resistance increasing with excess polymer dosage and higher charge density. However, the presence of polymer branches reduces floc resistance primarily due to larger floc size. Reflocculation is significantly improved with microparticles, particularly as floc strength decreases.

In industrial water with high cationic content, flocculation kinetics are enhanced, but the optimum flocculant dosage increases due to the more coiled polymer conformation and the presence of contaminants. Floc restructuring is less pronounced, with highly branched flocculants being less affected by water cationic content, resulting in similar floc structures regardless of the suspending medium.

In summary, highly branched flocculants exhibit consistent performance regardless of the water cationic content, highlighting the robustness of their floc structures across different environments.

Chapter 3

Flocculation process modelling

3.1 Introduction

The characteristics of flocs formed in the papermaking process, like in many other industries, play a critical role in determining the efficiency of the process and the quality of the final product. As previously detailed, the properties of flocs affect the retention of fines and fillers, water drainage, and sheet formation during the wet-end phase of paper production. Additionally, it has been established that the structure and size of flocs are influenced by the concentration of flocculants and the properties of the polymers used. Consequently, effective monitoring and management of these variables are essential for controlling floc size and structure throughout the flocculation process. To adequately understand, predict, and manage the flocculation of PCC particles by polyelectrolytes, a quantitative model capable of describing flocculation across various processing conditions is necessary. This chapter will delve deeper into the flocculation dynamics initiated by three medium charge density C-PAMs (E1, E1+, E1++++, and E2) discussed in Chapter 3. It is evident that floc reorganization stems from the reconformation of polymer chains at particle surfaces, primarily driven by a bridging mechanism induced by these polymers. This significant effect must be integrated into the modeling approach.

Population balance equations are fundamental to standard modeling techniques used to comprehend the dynamics of particulate systems. Generally, the most critical aspect characterizing the process in many applications is the distribution of particle sizes. This necessitates tracking particle counts as changes in particle populations translate to changes in system properties. The aim of this research is to develop a population balance model using Matlab® software to elucidate the flocculation of PCC particles via a bridging mechanism. This model is based on the discretized population balance equation (Equation 1.20), originally proposed by Spicer and Pratsinis (1996b) and Hounslow et al. (1988), which accounts for changes in particle size distribution over time.

$$\begin{aligned}\frac{dN_i}{dt} = &\sum_{j=1}^{i-2} 2^{j-i+1}\alpha_{i-1,j}\beta_{i-1,j}N_{i-1}N_j + \frac{1}{2}\alpha_{i-1,i-1}\beta_{i-1,i-1}N_{i-1}^2 \\ &- N_i\sum_{j=1}^{i-1} 2^{j-i}\alpha_{i,j}\beta_{i,j}N_j - N_i\sum_{j=i}^{\infty}\alpha_{i,j}\beta_{i,j}N_j - S_iN_i + \sum_{j=i}^{\infty}\Gamma_{i,j}S_jN_j\end{aligned} \tag{3.1}$$

Additionally, a predictive model will be developed to determine the properties of aggregates, such as size and structure, or to identify operating conditions that yield aggregates with desired characteristics for specific applications. This model will correlate various model parameters with polymer attributes (such as concentration and degree of branching). In Equation (1), N_i represents the number concentration of aggregates in the ith size interval, and N_1 represents the number concentration of primary particles. Each term on the right side of the equation corresponds to a different physical process:

- The first and second terms account for the formation of aggregates of size i from the combination of smaller aggregates.

- The third and fourth terms reflect the loss of aggregates of size i due to their incorporation into larger aggregates.

- The fifth term indicates the loss of aggregates of size i because of their breaking down into smaller aggregates.

- The sixth term represents the creation of smaller aggregates resulting from the breaking down of size i aggregates.

This structured approach in the equation helps in understanding the dynamic processes of aggregation and disintegration, crucial for optimizing the flocculation conditions in industrial applications.

3.2 Collision efficiency

The limitations inherent to the six principal assumptions of Smoluchowski are separately addressed in various models tailored to overcome specific challenges, as detailed in the literature, including Thomas (1999) on flocculation [56]. Adler [85] pioneered a model incorporating colloidal and hydrodynamic interactions, marking a significant development in understanding these dynamics. Further refining the modeling approaches, Han et al. [86] introduced a curvilinear method, offering adjustments to the earlier linear frameworks described by Li [87], though these models did not account for the porous characteristics of aggregates.

An alternative method to consider the impact of porosity in aggregates involves calculating the drag resulting from fluid flow through a porous sphere, as explored by Wu [88]. Additionally, Kusters et al. [89], advanced the field by applying trajectory analysis methods initially proposed by Adler [90] to study particle pathways more accurately.

Building on this foundation, Kusters et al. [79]formulated a model to quantify collision efficiency α using Equation (2), effectively integrating these various insights into a coherent framework that enhances our understanding of the flocculation process under diverse conditions. This comprehensive approach underscores the evolving complexity and sophistication in modeling flocculation dynamics, addressing previous assumptions and introducing more nuanced considerations of particle interactions.

$$\alpha_{ij} = \left[\frac{\exp\left(-x\left(1-\frac{i}{j}\right)^2\right)}{(i \times j)^y} \right] \times \alpha_{max} \tag{3.2}$$

The classes denoted by i and j are those in which colliding aggregates are located. x and y are fitting parameters and α_{max} is the upper limit of α_{ij}. As in the research of Selomulya et al. [78], Soos et al. [91] and Antunes et al. [92], we have taken into consideration x=y=0.1 in this work.Selomulya et al. [78] have shown that smaller values of x and y result in faster growth of the aggregates. The maximum collision efficiency value is an adjustable parameter as in the work of Soos et al. [91]

3.3 Collision frequency

The collision frequency, β_{ij}, can be due to Brownian motion and from orthokinetic aggregation [93] , as described in the equation below:

$$\beta_{ij} = \beta_{perkinetic} + \beta_{orthokinetic} \tag{3.3}$$

The collision frequency due to Brownian motion is given by Eq. (3.4) [94]where k_B is the Boltzmann constant, T is the absolute temperature and μ is the viscosity of the fluid.

$$\beta_{ij,\ perikinetic} = \left(\frac{2k_B T}{3\mu}\right) \frac{(R_{ci} + R_{cj})^2}{R_{ci} R_{cj}} \tag{3.4}$$

The collision frequency in isotropic turbulence for orthokinetic aggregation is given by Eq.(3.5) [95] where ε is the average energy dissipation rate and ν is the kinematic viscosity of the fluid.

$$\beta_{ij,\ orthokinetic} = 1.294 \left(\frac{\varepsilon}{\nu}\right)^{1/2} (R_{ci} + R_{cj})^3 \tag{3.5}$$

In Eqs. (3.4) and (3.5), Rc is the effective capture radius and, for fractal aggregates, it can be calculated from Eq. (6) [95] where r_0 is the primary particle radius, N is the number of primary particles in the aggregate, kc is a constant close to unity and d_F is the mass fractal dimension of the aggregate. The mass fractal dimension is a good way to quantify the aggregate structure with $1<d_F<3$ [61]. Lower fractal dimension values suggest structures that are extended and fragile, whereas higher values denote structures that are mechanically robust and densely packed [63]

$$R_{ci} = r_0 \left(\frac{N}{k_c}\right)^{1/d_F} \tag{3.6}$$

3.4 Fragmentation rate

The fragmentation rate, denoted as S_i, can be determined using the semi-empirical relation proposed by Kusters et al. (1997), expressed as in Equation 4. ε_{bi} represents the critical energy dissipation rate that causes break-up of flocs, while denotes the energy dissipation rate experienced by the flocs.

$$S_i = \left(\frac{4}{15\pi}\right)^{1/2} \left(\frac{\varepsilon}{\nu}\right)^{1/2} \exp\left(\frac{\varepsilon_{bi}}{\varepsilon}\right) \tag{3.7}$$

The experimental observations conducted by François in 1987, as documented in Eq. (8), revealed a significant relationship between the critical energy dissipation rate and the size of aggregates. Specifically, the equation indicates that larger aggregates demand less energy dissipation for breakage initiation, suggesting that larger flocs are more prone to fragmentation compared to smaller ones. Additionally, the findings suggest that as the shear rate $G = (\varepsilon/\nu)$ increases, the fragmentation rate also escalates. This correlation underscores the intricate interplay between aggregate size, energy dissipation, and shear rate, shedding

light on the mechanisms governing the breakage dynamics of flocs.

$$\varepsilon_{bi} = \frac{B}{R_{ci}} \tag{3.8}$$

B is a fitting parameter which allows to define at which size class i the flocs start to break up and with what intensity breakage occurs in this size class i for a given shear rate.

3.5 Breakage distribution function

B serves as a fitting parameter that enables the determination of the specific size class i at which flocs commence breakage and the magnitude of breakage intensity within this size category under a specified shear rate.

$$\begin{aligned} &\Gamma_{ij} = \frac{v_j}{v_i} \quad \text{for } j = i+1 \\ &\Gamma_{ij} = 0 \quad \text{for } j \neq i+1 \quad \text{where} \quad \begin{aligned} v_i &= 2^{i-1} v_0 \\ v_j &= 2^i v_0 \end{aligned} \end{aligned} \tag{3.9}$$

3.6 Flocs restructuring

The fractal dimension (dF), which characterizes the structure of flocs, undergoes changes over time. Consequently, the model introduced by Bonanomi et al. [96], as delineated by Eq. (10), offers a framework for elucidating the process of floc restructuring.

$$\frac{dd_F}{dt} = \gamma(d_{F,\max} - d_F) \tag{3.10}$$

In Equation 3.10, γ is defined as the restructuring rate, which acts as a fitting parameter, while $d_{F,\max}$ represents the highest value of the mass fractal dimension observed. For this research, due to the considerable size of the aggregates, the flocs' structure is more

accurately represented by the scattering exponent, SE, as noted in the works of [92, 23, 97]. Consequently, the scattering exponent SE is used in place of the mass fractal dimension, dF, to better align with the characteristics of the aggregates being studied.

3.7 Flocs size determination

From the floc size distribution, the parameter (d_{50}), also known as the median particle size, is often extracted. This value represents the particle size at which 50% of the distribution lies below it when calculated on a volume basis. Many researchers prefer to utilize the volume median size diameter in their investigations [98, 99]. This distribution type is particularly suitable for estimating self-preserving size distributions commonly encountered in aggregation processes [100].

Floc size was monitored using light diffraction scattering (LDS) with the Malvern Mastersizer 2000. The dispersion unit of the equipment contained 700 mL of distilled water into which the PCC suspension was added until 70% obscuration was achieved. To ensure good signal quality, obscuration was consistently maintained above 5% [82]. Floc size was monitored for a duration of 15 minutes, with size distribution data acquired every minute [101, 82]. The median size (volume-based) was extracted from the size distribution measured at each instant.

Additionally, by analyzing the scattered light intensity matrix offline, one can determine the average scattering exponent (SE) of the flocs at each moment of data acquisition, as detailed by Rasteiro et al. [102]. The SE is intimately linked to the structure of the flocs, notably their compactness, and this relationship is particularly significant in the context of large aggregates. This method allows for a deeper understanding of how floc structures evolve over time. Below is the flowchart illustrating the methodology used to solve the presented population balance model.

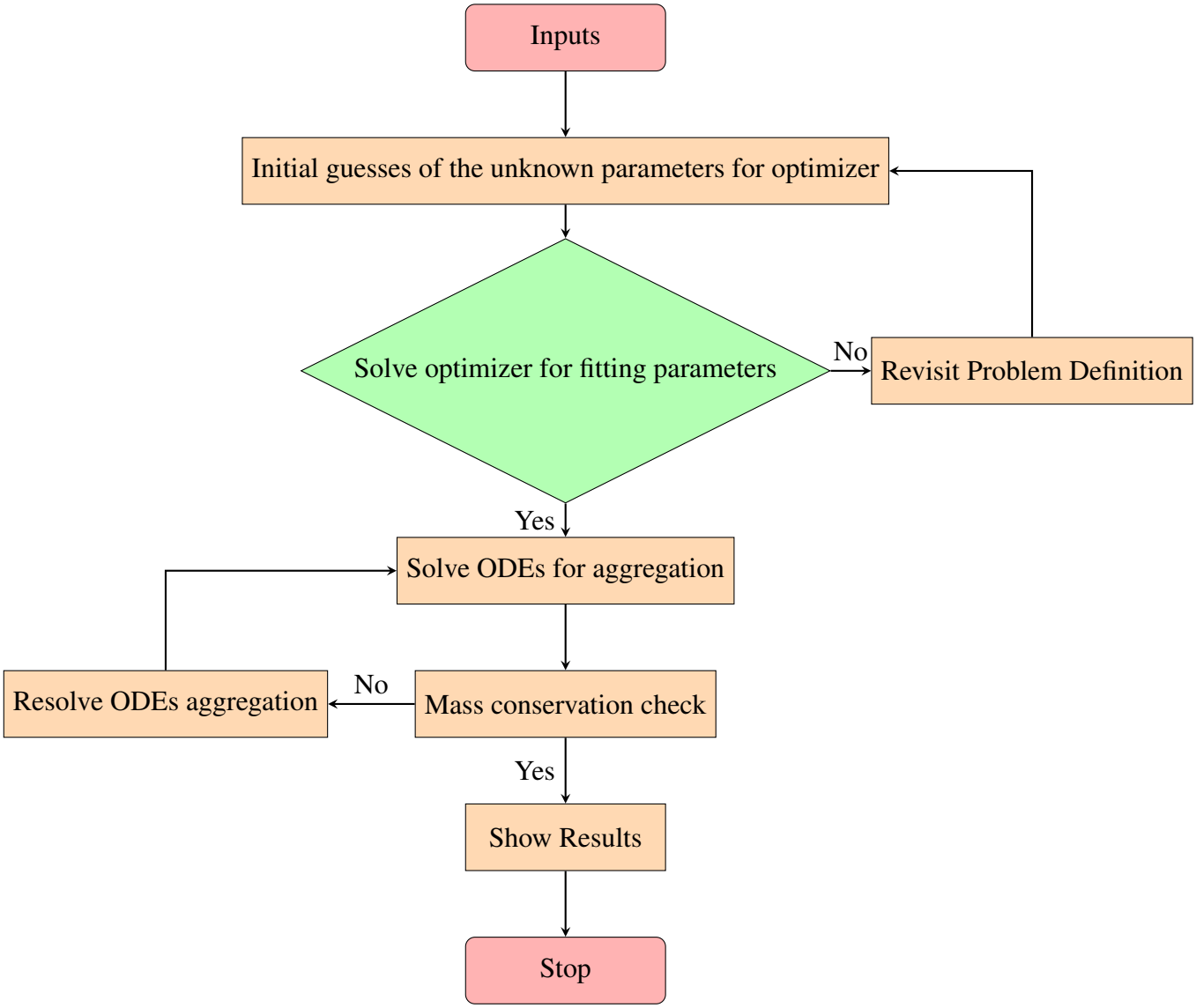

Fig. 3.1 Flowchart of the methodology for solving the PBEs.

3.8 Fixed pivot technique

The discretization methods applied by Kumar and Ramkrishna to handle both breakage and aggregation simultaneously utilize a consistent approach that incorporates the variables $N_i(t)s$ as used in earlier models. This consistency facilitates the integration of discrete equations for both processes into a cohesive set, leading to the formulation of the final equations as presented in their 1996 study. This integration simplifies the mathematical modeling of these complex processes, allowing for a more streamlined analysis.

$$\begin{aligned}\frac{dN_i(t)}{dt} = &\sum^{j\geq k}_{\substack{j,k \\ x_{i-1}\leq x_j+x_k\leq x_{i+1}}} \left(1-\tfrac{1}{2}\delta_{j,k}\right)\eta\,\alpha_{\mathrm{j,k}}\beta_{\mathrm{j,k}}\mathrm{N_j}(t)\mathrm{N_k}(t) \\ &-N_i(t)\textstyle\sum_{k=1}^{M}\alpha_{\mathrm{i,k}}\beta_{\mathrm{i,k}}N_k(t)+\sum_{k=i}^{M}n_{i,k}S_kN_k(t)-S_iN_i(t)\end{aligned} \tag{3.11}$$

Where δ represents the Dirac delta function, the quantity η is determined using straightforward expressions for maintaining both mass and number conservation.

$$\eta = \begin{cases} \frac{x_{i+1}-v}{x_{i+1}-x_i}, & x_i \leq v \leq x_{i+1} \\ \frac{v-x_{i-1}}{x_i-x_{i-1}}, & x_{i-1} \leq v \leq x_i \end{cases} \tag{3.12}$$

and $n_{i.k}$

$$n_{i.k} = \int_{x_i}^{x_{i+1}} \frac{x_{i+1}-v}{x_{i+1}-x_i}\sigma\left(v,x_k\right)dv + \int_{x_{i-1}}^{x} \frac{v-x_{i+1}}{x_i-x_{i-1}}\sigma\left(v,x_k\right)dv \tag{3.13}$$

$\sigma(v,x_k)dv$ denotes the number of daughter particles formed within the size range v to $v+dv$ resulting from the breakage of a larger particle of size k. The method offers several significant advantages: the derivation of the final equations is clear-cut, and the technique can accommodate more complex geometric grids such as $x_{i+1} = sx_i$, where $s > 1$, It can also integrate different grid types—for example, employing a consistently fine grid for smaller particle sizes combined with a geometric grid for larger sizes. This flexibility aids in assessing the convergence and accuracy of the numerical solutions by enabling minor adjustments

to the grids. A primary benefit, as identified by Kumar and Ramkrishna in 1996, is the method's ability to preserve any two properties in addition to number and mass, enhancing the versatility and applicability of the discretization technique in various contexts.

3.9 Solution of the model equations

A Matlab-based numerical solver was employed to implement the proposed population balance models, utilizing up to 30 intervals (imax=30) to cover the full range of aggregate sizes. The primary particles of precipitated calcium carbonate (PCC) used in the models had a standardized diameter of 0.1 mm. Consistency in modeling was maintained by assuming a constant shear rate (G) of 312 s^{-1}. Both the initial and maximum scattering exponents for the aggregates were individually determined based on experimental observations cited from Rasteiro et al. (2011).

The shear rate (G) inside the Mastersizer 2000 beaker was calculated using Computational Fluid Dynamics (CFD) simulations, conducted via COMSOL Multiphysics software as detailed in Antunes et al. (2010b). This was crucial due to the specific design of the beaker's shaft, which required precise characterization of flow dynamics. The average shear rate was used to describe the fluid motion within the beaker, as the velocity profiles showed uniform behavior across most areas, with only slight variations near the stirrer.

The stirring speed was set to match standard practice in papermaking flocculation. The initial concentration of particles (N for t=0) was calculated from the volume distribution data of the PCC particles obtained from the Mastersizer 2000. The research primarily investigated the flocculation of PCC using a range of cationic polyacrylamides (C-PAMs) with different molecular weights and charge densities, supplied by $AQUA+TECH$. The polymers used included Alpine-Floc E1+, Alpine-Floc E1, Alpine-Floc E1++++, which all had similar molecular weights but varied structurally, and Alpine-Floc E2, which featured a lower molecular weight and a linear structure.

The model fitting parameters $(\alpha_{max}, B, \gamma)$ were estimated using the method of minimum sum of squares clustering to accurately reflect changes in the volume median diameter, thereby optimizing the model's accuracy in simulating the flocculation process.

$$\min \psi_{\alpha_{\max},B,y} = \sum_{t=0}^{t=t_{\max}} \left(d_{50_{\text{expt}}} - d_{50_{\text{model}}}\right)^2 \tag{3.14}$$

3.10 Results and discussion

3.10.1 Flocculation kinetics: Experiment and simulation

All experimental scenarios were simulated using the two previously introduced models. Figures 4.1 and 4.2 display the flocculation kinetics observed experimentally alongside those predicted by the models for the four types of flocculants and three concentrations for each flocculant. The model-derived particle size distributions closely matched the experimental distributions within the same size range. Over time, the median floc size reaches its peak rapidly and then diminishes throughout the flocculation process. Across all flocculants examined, a concentration of 10mg/g PCC resulted in maximal flocculation and larger floc sizes, a trend confirmed by the models. The kinetics of flocculation varied based on polymer characteristics. High molecular weight linear polymers (E1) exhibited a sharper decline in the kinetic curve post-peak, whereas the decrease was less pronounced for lower molecular weight linear polymers (E2). This discrepancy is attributed to the arrangement of polymer molecules on particle surfaces, where linear polymers with higher molecular weights typically form more extended arrangements, yielding more porous flocs that are more prone to restructuring post-peak. Furthermore, the number of branches in the polymer chain influences the radius of gyration (Rg), with an increase in branching leading to a decrease in Rg and, consequently, a decrease in both floc restructuring and flocculation rate. The simulation models accurately capture this behavior. The optimal flocculant dosage,

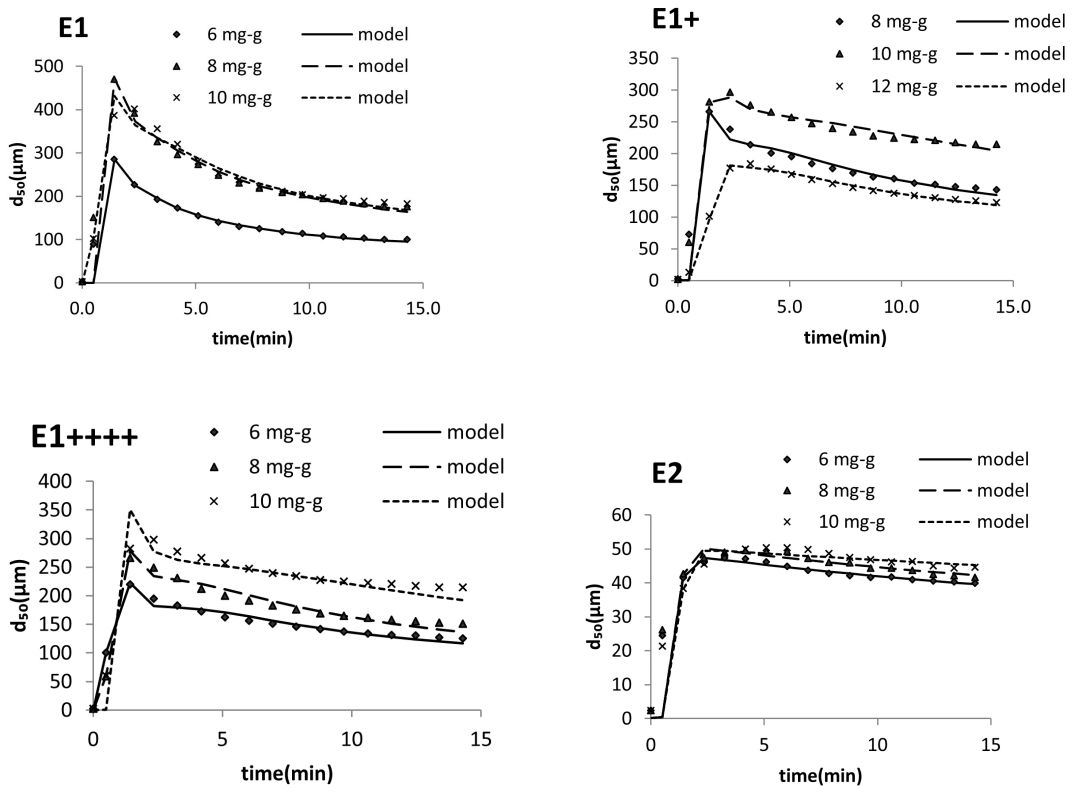

Fig. 3.2 . Experimental and modelled (Hounslow et al., 1988) flocculation kinetics for different flocculants and flocculant concentrations

characterized by larger floc sizes and faster flocculation rates, consistently stood at 10mg/g PCC across all tested polymers. Moreover, there was no significant disparity between the results (kinetic curves) obtained from either model. Notably, the average simulation time of the fixed pivot technique exceeded that of the Hounslow model.

3.11 Scattering Exponent

Figures 4.3 and 4.4 illustrate the evolution of the modeled floc structure, represented by the Scattering Exponent (SE), over time for various flocculants and concentrations, utilizing the Hounslow model and the fixed pivot method, respectively. Both models exhibit similar trends. Generally, larger discrepancies between experimental and calculated SE results are noted for

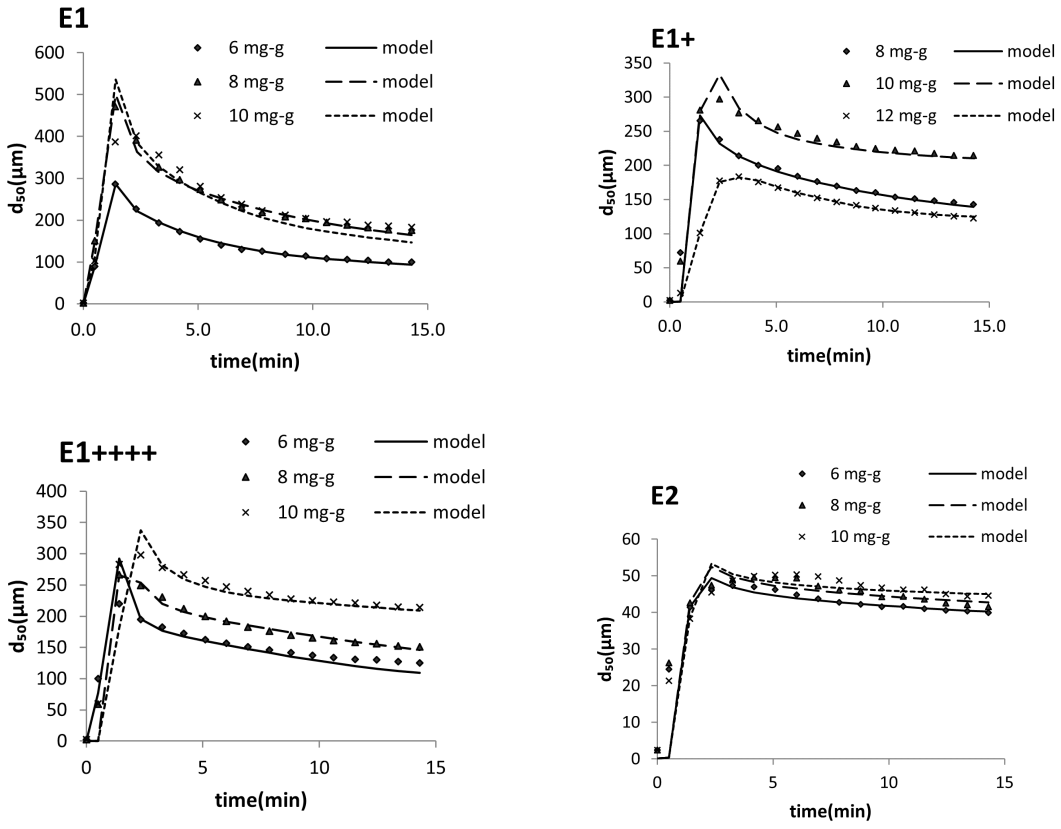

Fig. 3.3 Experimental and modelled (Fixed Pivot) flocculation kinetics for different flocculants and flocculant concentrations

higher flocculant concentrations, attributable to increased uncertainty in experimental values when larger, more porous flocs are formed. This uncertainty is compounded by the greater propensity for adhesion in such cases, given the available light scattering signal treatment model. Moreover, larger deviations between experimental and calculated values are observed at the initial stages of flocculation.

Across all cases, the scattering exponent attains its minimum values at concentrations leading to larger flocs (10mg/g), indicative of the dominant bridging mechanism, leading to bigger and more loosely structured flocs. The rapid increase in the scattering exponent until reaching a maximum during floc restructuring underscores the significance of this process in yielding more compact flocs.

For the E2 flocculant, which is a lower molecular weight linear polymer, changes in the scattering exponent (SE) over time are minimal due to almost negligible restructuring. This observation is in line with the possibility of combining both bridging and patching mechanisms in the flocculation processes when using lower molecular weight polymers for particle aggregation. As a result, there is a closer correspondence between the experimental results and the SE values calculated through modeling in this case. Furthermore, when using the E1 polymer for flocculation, the final SE at a concentration of 10 mg/g exceeds that seen with other high molecular weight polymers in the E1 series, which correlates with achieving smaller floc sizes after restructuring with this particular polymer.

3.12 Optimized PBM Model Parameters

Table 1 presents the optimized parameters along with the statistical measures of the models' fit. To evaluate how well the models align with the experimental data, a goodness of fit parameter is calculated using equation (15), as detailed by Biggs and Lant [103].

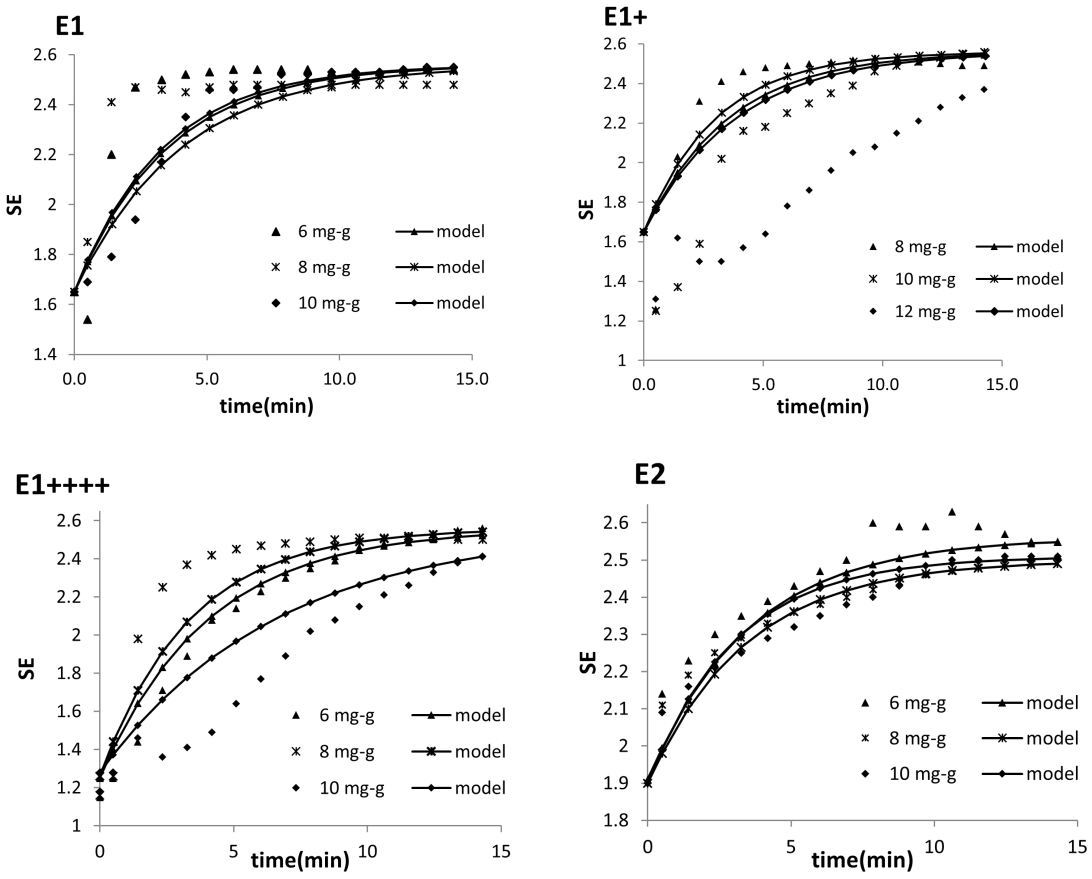

Fig. 3.4 Experimental and modelled (Hounslow et al., 1988) scattering exponent variation for different flocculants and flocculant concentrations

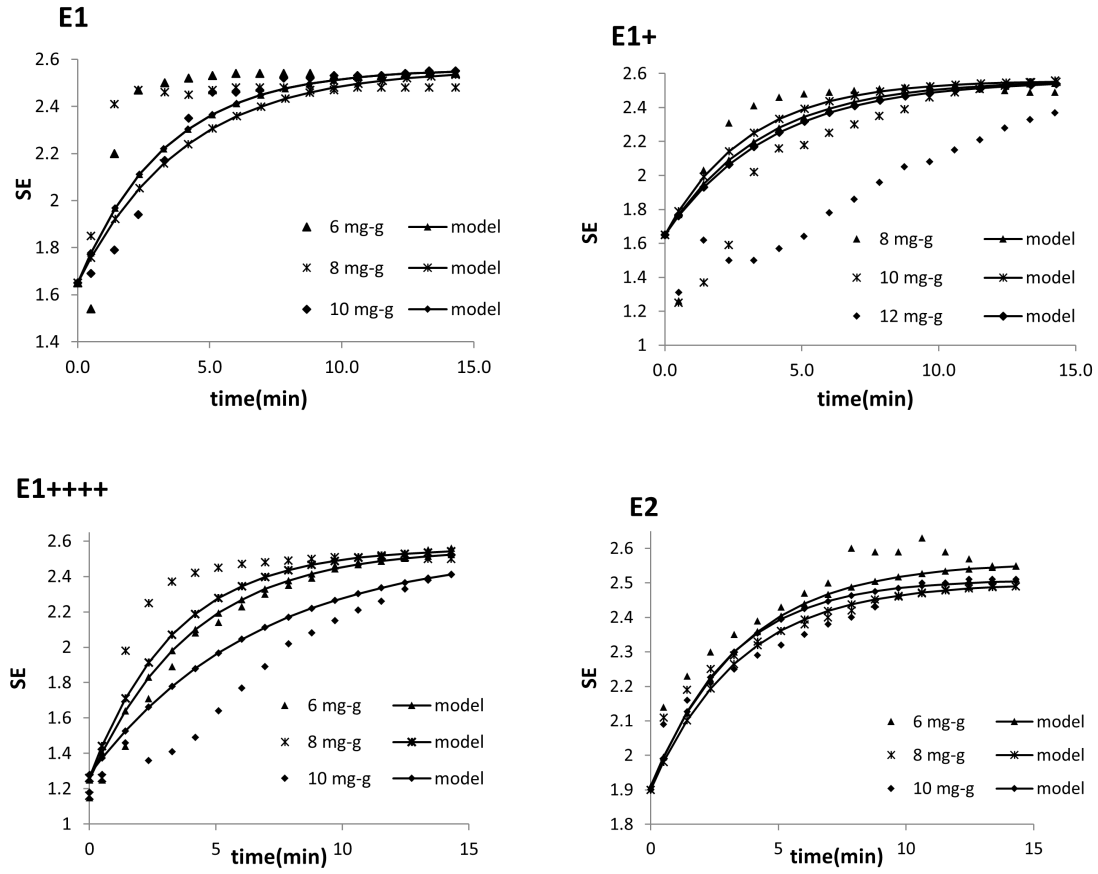

Fig. 3.5 Experimental and modelled (Fixed Pivot) scattering exponent variation for different flocculants and flocculant concentrations

$$\mathrm{GoF}(\%) = 100\frac{\left\langle d_{\mathrm{agg.exp}} \right\rangle - std}{\left\langle d_{\mathrm{agg.exp}} \right\rangle} \tag{3.15}$$

$$std = \left(\frac{1}{n-f} \sum_{t_i}^{t_f} \left(\left\langle d_{\mathrm{agg.exp}} \right\rangle - \left\langle d_{\mathrm{agg.mod}} \right\rangle \right)^2 \right)^{\frac{1}{2}} \tag{3.16}$$

Where std represents the standard deviation, n denotes the number of data values, and f signifies the number of parameters to be fitted. There were no significant disparities observed between the results of the two models, and a robust fitting, with a goodness-of-fit (Gof) exceeding 98% in all instances, corroborates the suitability of the models for predicting the flocculation process based on the bridging mechanism. This mechanism entails the polymer's adsorption onto particle surfaces with extended conformation, leading to the formation of tails and loops that extend beyond the electrical double layer. Consequently, these extensions link with other particles, facilitating the aggregation of PCC particles [1]. The parameter B serves as an indicator of the fragmentation rate, increasing for larger floc sizes, as larger flocs are more prone to breakage. Simultaneously, as B increases, other parameters generally decrease. Additionally, floc restructuring becomes more pronounced (as indicated by higher γ when polymer chain reconformation on particle surfaces is more extensive. Lower γ values were observed for polymer E2, a lower molecular weight polymer less inclined towards reconformation, likely inducing a combination of bridging and patching flocculation mechanisms.

Furthermore, the fitting parameters presented in Table 1 affirm that, for polymers of the same molecular weight, lower γ values (related to floc restructuring) are obtained when the polymer is branched, reflecting the greater difficulty of polymer reconformation on particle surfaces for branched polymers.

According to Figure 3 and Table 1, there is a clear relationship where an increase in parameter B is associated with a reduction in the scattering exponent. This suggests that

Table 3.1 Optimum fitting parameters for E1, E2, E1+ and E1++++ (three parameters model) using either the Hounslow model or the Fixed Pivot technique

Flocculant	Dosage (mg/g)	α_{max}		β		γ		GoF(%)	
		Hounslow	FP	Hounslow	FP	Hounslow	FP	Hounslow	FP
E1	6	0.261	0.409	37.68	33.38	0.056	0.044	98.85	99.88
	8	0.229	0.354	55.66	46.96	0.037	0.025	98.87	99.75
	10	0.283	0.286	55.55	50.84	0.035	0.042	99.76	98.81
E2	6	0.969	0.951	8.86	7.82	0.007	0.003	98.95	98.94
	8	0.914	0.884	9.10	8.35	0.007	0.003	98.94	98.92
	10	0.876	0.855	9.09	8.45	0.003	2E-4	99.13	99.08
E1+	8	0.162	0.990	40.56	35.68	0.021	0.018	99.25	99.11
	10	0.142	0.164	49.67	43.68	0.011	4E-5	99.58	99.35
	12	0.146	0.255	35.52	73.39	0.019	0.247	99.76	99.82
E1++++	6	0.333	0.330	35.26	31.00	0.022	0.019	99.86	99.39
	8	0.307	0.156	41.66	37.18	0.025	0.015	99.93	99.38
	10	0.258	0.134	47.88	44.68	0.016	0.006	99.15	98.66

larger flocs, which tend to have more open structures, are more prone to breakage, a finding that aligns with results from earlier research [102].

Conclutions

This research highlights the utility of the Light Diffraction Scattering (LDS) method in analyzing and comprehending the flocculation process, as well as precisely identifying floc properties. The pioneering experimental approach used enables the detailed, single-session collection of data on the changes in floc size and structure throughout the process, as well as assessments of floc resistance and flocculation kinetics. This marks a significant improvement over traditional methods like titration, image analysis, and turbidity measurements for studying flocculation.

These studies are essential for understanding floc resistance under conditions typical of various industrial processes, such as those found in papermaking. The approach has also facilitated the evaluation of dual retention aids, enhancing the performance of flocculants in conjunction with microparticles.The flocculant characteristics, particularly the variations in charge density and molecular structure from linear to highly branched polymers, have significant implications for floc formation and are crucial for optimizing process performance.

The findings affirm that LDS is an invaluable tool for gauging the effectiveness of polymeric flocculants across both simple and complex flocculation systems, surpassing traditional methods in determining floc characteristics. Additionally, the methodology could be readily adapted to other flocculation systems to predict and enhance flocculant performance, despite some limitations related to maximum solids concentration which may not align with industrial scales.This comprehensive approach is promising for refining flocculation processes in papermaking, highlighting that medium charge density polymers,

especially branched ones, are particularly beneficial as retention aids due to their efficient performance in forming desirable floc structures.

In this study, two distinct approaches for population balance modeling were employed to elucidate the flocculation dynamics of precipitated calcium carbonate when treated with cationic polyacrylamides (C-PAMs) showcasing varied characteristics. These methodologies include the approach delineated by Hounslow et al. [72] and Spicer et al. [55], alongside the fixed pivot technique introduced by Kumar et al. [80]. This investigation uniquely contrasts these models within the realm of paper manufacturing-related flocculation processes, marking a novel endeavor according to the authors' awareness. Both modeling techniques effectively capture the concurrent phenomena of aggregation and disintegration, offering a reliable approximation of the flocs' volume median size evolution over time. Despite employing a consistent grid for analysis, the models produced similar outcomes, albeit the fixed pivot method necessitated an extended simulation duration. The models demonstrated a high degree of accuracy in mimicking experimental observations, with a goodness of fit (GoF) surpassing 98% across all scenarios. Through fitting parameter analysis, insightful details on critical aspects of the flocculation process, including fragmentation rate, collision efficiency, and floc restructuring across various flocculant specifications and dosages, were revealed. The models showcased their effectiveness particularly in scenarios where the bridging mechanism was prevalent, enabling an analytical comparison of operational conditions to achieve specific performance benchmarks.

References

[1] A Blanco, E Fuente, C Negro, and J Tijero. Flocculation monitoring: focused beam reflectance measurement as a measurement tool. *The Canadian Journal of Chemical Engineering*, 80(4):1–7, 2002.

[2] M Nurmi, M Westerholm, and D Eklund. Factors influencing flocculation of dissolved and colloidal substances in a thermomechanical pulp water. *Journal of pulp and paper science*, 30(2):41–44, 2004.

[3] V-M Hulkko and Yulin Deng. Effects of water-soluble inorganic salts and organic materials on the performance of different polymer retention aids. *Journal of pulp and paper science*, 25(11):378–383, 1999.

[4] Myriam Cadotte, Marie-Eve Tellier, Angeles Blanco, Elena Fuente, Theo GM Van De Ven, and Jean Paris. Flocculation, retention and drainage in papermaking: a comparative study of polymeric additives. *The Canadian Journal of Chemical Engineering*, 85(2):240–248, 2007.

[5] Patrick T Spicer, Sotiris E Pratsinis, Judy Raper, Rose Amal, Graeme Bushell, and Gabrie Meesters. Effect of shear schedule on particle size, density, and structure during flocculation in stirred tanks. *Powder Technology*, 97(1):26–34, 1998.

[6] Ad A Berlin and VN Kislenko. Kinetic models of suspension flocculation by polymers. *Colloids and Surfaces A: Physicochemical and Engineering Aspects*, 104(1):67–72, 1995.

[7] Kristen E Bremmell, GJ Jameson, and S Biggs. Polyelectrolyte adsorption at the solid/liquid interface: interaction forces and stability. *Colloids and Surfaces A: Physicochemical and Engineering Aspects*, 139(2):199–211, 1998.

[8] Simon Biggs, Michael Habgood, Graeme J Jameson, et al. Aggregate structures formed via a bridging flocculation mechanism. *Chemical Engineering Journal*, 80(1-3):13–22, 2000.

[9] T Asselman and G Garnier. The flocculation mechanism of microparticulate retention aid systems. *Journal of pulp and paper science*, 27(8):273–278, 2001.

[10] Roger Nyström, Gun Hedström, Jan Gustafsson, and Jarl B Rosenholm. Mixtures of cationic starch and anionic polyacrylate used for flocculation of calcium carbonate—influence of electrolytes. *Colloids and Surfaces A: Physicochemical and Engineering Aspects*, 234(1-3):85–93, 2004.

[11] J. Gregory. The action of polymeric flocculants in flocculation, sedimentation and consolidation. *Acta. Math.*, 158:125–137, 1985. Conference 1985, Sea Island, GA, USA, 27 January–1 February 1985.

[12] Sara Stemme, Lars Ödberg, and Martin Malmsten. Effect of colloidal silica and electrolyte on the structure of an adsorbed cationic polyelectrolyte layer. *Colloids and Surfaces A: Physicochemical and Engineering Aspects*, 155(2-3):145–154, 1999.

[13] Agne Swerin, Ulf Sjödin, and Lars Odberg. Flocculation of cellulosic fibre suspensions by model microparticulate retention aid systems: effect of polymer charge density and type of microparticle. *Nordic Pulp & Paper Research Journal*, 8(4):389–398, 1993.

[14] Takanori Miyanishi. Optimizing flocculation and drainage for microparticle systems by controlling zeta potential. *Tappi journal*, 80(1):262, 1997.

[15] C Negro, E Fuente, A Blanco, and J Tijero. Flocculation mechanism induced by phenolic resin/peo and floc properties. *AIChE journal*, 51(3):1022–1031, 2005.

[16] TG M van de Ven and B Alince. Association-induced polymer bridging: new insights into the retention of fillers with peo. *Journal of pulp and paper science*, 22(7):J257–J263, 1996.

[17] F Brouillette, D Morneau, B Chabot, and C Daneault. Polyacrylics paper formation improvement through the use of new structured polymers and microparticle technology. *PULP AND PAPER CANADA-ONTARIO-*, 105:31–35, 2004.

[18] J-H Shin, Sin Ho Han, Changman Sohn, Say Kyoun Ow, and Soukil Mah. Highly branched cationic polyelectrolytes: Fines retention. *Tappi journal*, 80(10):185–189, 1997.

[19] AJ Dunham, LM Sherman, and JC Alfano. Effect of dissolved and colloidal substances on drainage properties of mechanical pulp suspensions. *Journal of pulp and paper science*, 28(9):298–304, 2002.

[20] JC Alfano, PW Carter, and JE Whitten. Use of scanning laser microscopy to investigate microparticle flocculation performance. *Journal of pulp and paper science*, 25(6):189–195, 1999.

[21] Victor Shubin and Per Linse. Self-consistent-field modeling of polyelectrolyte adsorption on charge-regulating surfaces. *Macromolecules*, 30(19):5944–5952, 1997.

[22] A Blanco, C NEGRO, I SAN PIO, J Tijero, et al. Monitoring flocculation of fillers in papermaking. *Paper technology (1989)*, 44(8):41–50, 2003.

[23] MY Lin, RUDOLF Klein, HM Lindsay, DAVID A Weitz, ROBIN C Ball, and PAUL Meakin. The structure of fractal colloidal aggregates of finite extent. *Journal of colloid and interface science*, 137(1):263–280, 1990.

[24] William E Scott. *Principles of wet end chemistry*. Tappi Press, 1996.

[25] Francois Brouillette, Bruno Chabot, Daniel Morneau, and Claude Daneault. A new microparticulate system to improve retention/drainage in fine paper manufacturing. *Appita: Technology, Innovation, Manufacturing, Environment*, 58(1):47–51, 2005.

[26] Pedro Fardim. Papel e química de superfície-parte i–a superfície da fibra e a química da parte úmida. *O Papel, São Paulo*, (4):97–107, 2002.

[27] Angeles Blanco, Carlos Negro, Elena Fuente, and Julio Tijero. Effect of shearing forces and flocculant overdose on filler flocculation mechanisms and floc properties. *Industrial & engineering chemistry research*, 44(24):9105–9112, 2005.

[28] Gary A Smook. Handbook for pulp and paper technologists. angus wilde publications. *Inc., Canada*, 1992.

[29] Margaret A Dulany, George L Batten Jr, Michael C Peck, and Charles E Farley. Papermaking additives. *Kirk-Othmer Encyclopedia of Chemical Technology*, 2000.

[30] A Blanco. *Estudio de la floculación en la fabricación de papel*. PhD thesis, PhD. Thesis, Universidad Complutense, Madrid, Spain, 1994.

[31] MA Blanco, J Tijero, and A Hooimeijer. Study of flocculation process in papermaking. In *PAPERMAKERS CONFERENCE*, pages 455–455. TAPPI PRESS, 1995.

[32] Dan Eklund and Tom Lindström. *Paper chemistry: an introduction*. DT Paper Science Publications, 1991.

[33] JE Unbehend. Wet end chemistry of retention, drainage and formation aids. *Pulp and Paper Manufacture*, 6:112–157, 1992.

[34] RH Pelton, BD Jordan, and LH Allen. Particle size distributions of fines in mechanical pulps and some aspects of their retention in papermaking. *Tappi journal*, 68(2):91–94, 1985.

[35] Kari Luukko and Hannu Paulapuro. Mechanical pulp fines: Effect of particle size and shape. *Tappi journal*, 82(2):95–101, 1999.

[36] Maria Norell, Kjell Johansson, and Michael Persson. Retention and drainage, 1999.

[37] M Stén. Importance of papermaking chemistry. *Papermaking Science and Technology, Book*, 4:12–17, 1999.

[38] Ben Pruden. The effect of fines on paper properties. *Paper technology (1989)*, 46(4):19–26, 2005.

[39] KW Britt, JE Unbehend, and R Shridharan. Observations on water removal in papermaking. *Tappi journal*, 69(7):76–79, 1986.

[40] VJ Wildfong, JM Genco, JA Shands, and DW Bousfield. Filtration mechanics of sheet forming. part i: Apparatus for determination of constant-pressure filtration resistance. *Journal of pulp and paper science*, 26(7):250–254, 2000.

[41] Mark A Paradis, Joseph M Genco, Douglas W Bousfield, John C Hassler, and Vaughn Wildfong. Determination of drainage resistance coefficients under known shear rate. *Tappi J*, 1(8):12–18, 2002.

[42] Edward Litchfield. Dewatering aids for paper applications. *Appita*, 47(1):62–65, 1994.

[43] Peter Jarvis, Bruce Jefferson, JOHN Gregory, and Simon A Parsons. A review of floc strength and breakage. *Water research*, 39(14):3121–3137, 2005.

[44] P.C. Hiemenz and R. Rajagopalan. *Principles of Colloid and Surface Chemistry, Third Edition, Revised and Expanded*. Undergraduate Chemistry: A Series of Textbooks. Taylor & Francis, 1997.

[45] Ad A Berlin, IM Solomentseva, and VN Kislenko. Suspension flocculation by polyelectrolytes: Experimental verification of a developed mathematical model. *Journal of colloid and interface science*, 191(2):273–276, 1997.

[46] Xiang Yu and P Somasundaran. Enhanced flocculation with double flocculants. *Colloids and Surfaces A: Physicochemical and Engineering Aspects*, 81:17–23, 1993.

[47] Aixing Fan, Nicholas J Turro, and P Somasundaran. A study of dual polymer flocculation. *Colloids and surfaces a: physicochemical and engineering aspects*, 162(1-3):141–148, 2000.

[48] CH Lee and JC Liu. Sludge dewaterability and floc structure in dual polymer conditioning. *Advances in Environmental Research*, 5(2):129–136, 2001.

[49] Se-Young Yoon and Yulin Deng. Flocculation and reflocculation of clay suspension by different polymer systems under turbulent conditions. *Journal of colloid and interface science*, 278(1):139–145, 2004.

[50] A Swerin, G Risinger, and L Ödberg. Flocculation in suspensions of microcrystalline cellulose by microparticle retention aid systems. *Journal of pulp and paper science*, 23(8):J374–J381, 1997.

[51] Tom Lindström and Gunborg Glad-Nordmark. Network flocculation and fractionation of latex particles by means of a polyethyleneoxide—phenolformaldehyde resin complex. *Journal of colloid and interface science*, 97(1):62–67, 1984.

[52] Tharwat F Tadros. *Applied surfactants: principles and applications*. John Wiley & Sons, 2006.

[53] M Hermawan, T Yang, G Bushell, R Amal, and G Bickert. A new approach in determining floc strength. *Part. Syst. Anal., Harrogate, UK*, 2003.

[54] Denny S Parker, Warren J Kaufman, and David Jenkins. Floc breakup in turbulent flocculation processes. *Journal of the Sanitary Engineering Division*, 98(1):79–99, 1972.

[55] Patrick T Spicer and Sotiris E Pratsinis. Coagulation and fragmentation: Universal steady-state particle-size distribution. *AIChE journal*, 42(6):1612–1620, 1996.

[56] DN Thomas, SJ Judd, and N Fawcett. Flocculation modelling: a review. *Water research*, 33(7):1579–1592, 1999.

[57] Mehmet Ali Yukselen and John Gregory. The reversibility of floc breakage. *International Journal of Mineral Processing*, 73(2-4):251–259, 2004.

[58] Anthony KC Yeung and Robert Pelton. Micromechanics: a new approach to studying the strength and breakup of flocs. *Journal of Colloid and Interface Science*, 184(2):579–585, 1996.

[59] Serge Stoll and Pierre Chodanowski. Polyelectrolyte adsorption on an oppositely charged spherical particle. chain rigidity effects. *Macromolecules*, 35(25):9556–9562, 2002.

[60] Daniel Solberg and Lars Wågberg. Adsorption and flocculation behavior of cationic polyacrylamide and colloidal silica. *Colloids and Surfaces A: Physicochemical and Engineering Aspects*, 219(1-3):161–172, 2003.

[61] Rajat K Chakraborti, Kevin H Gardner, Joseph F Atkinson, and John E Van Benschoten. Changes in fractal dimension during aggregation. *Water Research*, 37(4):873–883, 2003.

[62] Sharna M Glover, Graeme J Jameson, Simon Biggs, et al. Bridging flocculation studied by light scattering and settling. *Chemical Engineering Journal*, 80(1-3):3–12, 2000.

[63] Graeme Bushell. Forward light scattering to characterise structure of flocs composed of large particles. *Chemical Engineering Journal*, 111(2-3):145–149, 2005.

[64] GC Bushell, YD Yan, D Woodfield, JUDY Raper, and ROSE Amal. On techniques for the measurement of the mass fractal dimension of aggregates. *Advances in Colloid and Interface Science*, 95(1):1–50, 2002.

[65] BS ISO. 13320-1 (1999). particle size analysis-laser diffraction methods-part 1: General principles. *British Standards Institution, London*, 1999.

[66] Gerben BJ de Boer, Cornelis de Weerd, Dirk Thoenes, and Hendrik WJ Goossens. Laser diffraction spectrometry: Fraunhofer diffraction versus mie scattering. *Particle & Particle Systems Characterization*, 4(1-4):14–19, 1987.

[67] Agne Swerin. Rheological properties of cellulosic fibre suspensions flocculated by cationic polyacrylamides. *Colloids and Surfaces A: Physicochemical and Engineering Aspects*, 133(3):279–294, 1998.

[68] RJ Kerekes, RM Soszynski, and Tam Doo. The flocculation of pulp fibres. In *Papermaking Raw Materials: Their Interaction with the Production Process and Their Effect on Paper Properties-Transactions of the Eighth Fundamental Research Symposium held at Oxford: September 1985*, pages 265–310, 1985.

[69] Agne Swerin, Robert L Powell, and Lars Odberg. Linear and nonlinear dynamic viscoelasticity of pulp fiber suspensions. *Nordic Pulp & Paper Research Journal*, 7(3):126–132a, 1992.

[70] Tie-Qiang Li and Lars Ödberg. Flow properties of cellulose fiber suspensions flocculated by cationic polyacrylamide. *Colloids and Surfaces A: Physicochemical and Engineering Aspects*, 115:127–135, 1996.

[71] Carlos Negro, Elena Fuente, Angeles Blanco, and Julio Tijero. Effect of chemical flocculation mechanisms on rheology of fibre pulp suspensions. *Nordic Pulp & Paper Research Journal*, 21(3):336–341, 2006.

[72] MJ Hounslow, RL Ryall, and VR Marshall. A discretized population balance for nucleation, growth, and aggregation. *AIChE journal*, 34(11):1821–1832, 1988.

[73] Gordon M Fair and Robert S Gemmell. A mathematical model of coagulation. *Journal of Colloid Science*, 19(4):360–372, 1964.

[74] Ruben D Cohen. The self-similar cluster size distribution in random coagulation and breakup. *Journal of colloid and interface science*, 149(1):261–270, 1992.

[75] Margaritis Kostoglou, S Dovas, and AJ Karabelas. On the steady-state size distribution of dispersions in breakage processes. *Chemical Engineering Science*, 52(8):1285–1299, 1997.

[76] Alex R Heath, Parisa A Bahri, Phillip D Fawell, and John B Farrow. Polymer flocculation of calcite: Population balance model. *AIChE Journal*, 52(5):1641–1653, 2006.

[77] Jürgen C Flesch, Patrick T Spicer, and Sotiris E Pratsinis. Laminar and turbulent shear-induced flocculation of fractal aggregates. *AIChE journal*, 45(5):1114–1124, 1999.

[78] Cordelia Selomulya, Graeme Bushell, Rose Amal, and T DAVID Waite. Understanding the role of restructuring in flocculation: The application of a population balance model. *Chemical Engineering Science*, 58(2):327–338, 2003.

[79] Karl A Kusters, Johan G Wijers, and Dirk Thoenes. Aggregation kinetics of small particles in agitated vessels. *Chemical Engineering Science*, 52(1):107–121, 1997.

[80] Sanjeev Kumar and Doraiswami Ramkrishna. On the solution of population balance equations by discretization—i. a fixed pivot technique. *Chemical Engineering Science*, 51(8):1311–1332, 1996.

[81] MG Rasteiro, FAP Garcia, and M del Mar Peréz. Applying lds to monitor flocculation in papermaking. *Particulate Science and Technology*, 25(3):303–308, 2007.

[82] MG Rasteiro, FAP Garcia, P Ferreira, A Blanco, C Negro, and E Antunes. The use of lds as a tool to evaluate flocculation mechanisms. *Chemical Engineering and Processing: Process Intensification*, 47(8):1323–1332, 2008.

[83] Elisabete Antunes, Fernando AP Garcia, Paulo Ferreira, Angeles Blanco, Carlos Negro, and M Graça Rasteiro. Use of new branched cationic polyacrylamides to improve retention and drainage in papermaking. *Industrial & Engineering Chemistry Research*, 47(23):9370–9375, 2008.

[84] TGM Van de Ven and B Alince. Heteroflocculation by asymmetric polymer bridging. *Journal of colloid and interface science*, 181(1):73–78, 1996.

[85] PM Adler. Heterocoagulation in shear flow. *Journal of Colloid and Interface Science*, 83(1):106–115, 1981.

[86] Mooyoung Han and Desmond F Lawler. The (relative) insignificance of g in flocculation. *Journal-American Water Works Association*, 84(10):79–91, 1992.

[87] Xiaoyan Li and Bruce E Logan. Collision frequencies between fractal aggregates and small particles in a turbulently sheared fluid. *Environmental science & technology*, 31(4):1237–1242, 1997.

[88] RM Wu and DJ Lee. Hydrodynamic drag force exerted on a moving floc and its implication to free-settling tests. *Water Research*, 32(3):760–768, 1998.

[89] Karl A Kusters, JG Wijers, and D Thoenes. Numerical particle tracking in a turbine agitated vessel. In *Fluid Mechanics of Mixing: Modelling, Operations and Experimental Techniques*, pages 233–245. Springer, 1992.

[90] PM Adler. Streamlines in and around porous particles. *Journal of Colloid and Interface Science*, 81(2):531–535, 1981.

[91] Miroslav Soos, Jan Sefcik, and Massimo Morbidelli. Investigation of aggregation, breakage and restructuring kinetics of colloidal dispersions in turbulent flows by population balance modeling and static light scattering. *Chemical engineering science*, 61(8):2349–2363, 2006.

[92] E Antunes, P Ferreira, MG Rasteiro, and FAP Garcia. Evaluation of polyelectrolyte performance on pcc flocculation using the lds technique. *Particulate Science and Technology*, 28(5):426–441, 2010.

[93] David L Swift and S_K_ Friedlander. The coagulation of hydrosols by brownian motion and laminar shear flow. *Journal of colloid science*, 19(7):621–647, 1964.

[94] M von Smoluchowski. Study of a mathematical theory of the coagulation kinetics of colloidal solutions. *Z. Phys. Chem.*, 92:129, 1917.

[95] PGF Saffman and JS Turner. On the collision of drops in turbulent clouds. *Journal of Fluid Mechanics*, 1(1):16–30, 1956.

[96] Eleonora Bonanomi, Jan Sefcik, Manfred Morari, and Massimo Morbidelli. Analysis and control of a turbulent coagulator. *Industrial & engineering chemistry research*, 43(19):6112–6124, 2004.

[97] Cordelia Selomulya, Graeme Bushell, Rose Amal, and TD Waite. Aggregation mechanisms of latex of different particle sizes in a controlled shear environment. *Langmuir*, 18(6):1974–1984, 2002.

[98] Jie Chen, Xiaojun Xu, Rui Nie, Li Feng, Xuhao Li, and Bingzhi Liu. Chitosan modified cationic polyacrylamide initiated by uv-h2o2 for sludge flocculation and new insight on the floc characteristics study. *Polymers*, 12(11):2738, 2020.

[99] RB Moruzzi, John Bridgeman, and PAG Silva. A combined experimental and numerical approach to the assessment of floc settling velocity using fractal geometry. *Water Science and Technology*, 81(5):915–924, 2020.

[100] CM Sorensen, N Lu, and J Cai. Fractal cluster size distribution measurement using static light scattering. *Journal of Colloid and Interface Science*, 174(2):456–460, 1995.

[101] E Antunes, FAP Garcia, P Ferreira, A Blanco, C Negro, and MG Rasteiro. Modelling pcc flocculation by bridging mechanism using population balances: Effect of polymer characteristics on flocculation. *Chemical Engineering Science*, 65(12):3798–3807, 2010.

[102] Maria G Rasteiro, Ineide Pinheiro, Fernando AP Garcia, Paulo Ferreira, and David Hunkeler. Using light scattering to screen polyelectrolytes (pel) performance in flocculation. *Polymers*, 3(2):915–927, 2011.

[103] CA Biggs and PA Lant. Modelling activated sludge flocculation using population balances. *Powder Technology*, 124(3):201–211, 2002.